Reviewed Preprint
v1 • May 14, 2026
Not revised

For correspondence:
Frieder.schoeck@mcgill.ca

Competing interests: No competing interests declared

Funding: See page 22

Reviewing editor: Michael Buszczak, University of Texas Southwestern Medical Center, United States

Zasp52's differentially expressed intrinsically disordered region confers thin filament stability at the Z-disc

Nikolai Ho, Frieder Schöck
Department of Biology, McGill University, Montreal, Canada

eLife Assessment

This study investigates the role of the Z-disc protein Zasp52 in Drosophila flight muscles and provides evidence that an intrinsically disordered region (IDR) helps to stabilize and promote the localization of the protein to the Z-disc. Overall, this represents an **important** study that provides insights into Z-disc function and maintenance. The data are **convincing**, supported by strong genetic evidence and behavioral tests, well-controlled experiments, and detailed statistical analyses. Additional functional analyses designed to tease out specialized regions within the newly described isoform of Zasp52 would further strengthen models regarding the function of the protein.

https://doi.org/10.7554/eLife.111101.1.sa3

Abstract

The Drosophila scaffolding protein Zasp52 is required to maintain structure at the muscle Z-disc which experiences strong forces during contraction. It is alternatively spliced into many isoforms, some of which contain a long intrinsically disordered region (IDR). We show that this region is primarily expressed in the indirect flight muscle (IFM) and is required for maintaining integrity of the Z-disc. Deleting the IDR-encoding exon15e results in flightlessness and structural IFM defects, including sarcomere bending at the Z-disc and an inability to de-contract. These defects are indicative of a lack of proper thin filament anchoring to the Z-disc. This is further supported by a genetic interaction between exon15e and actin. Fluorescence recovery after photobleaching of an isoform lacking exon15e shows that the IDR is required for maintaining Zasp52 at the Z-disc and thereby stabilizing Z-discs. Lastly, we can rescue these phenotypes by restricting IFM use. Together, these results suggest that Zasp52's IDR confers thin filament stability at the Z-disc of IFM.

Background

The fruit fly *Drosophila melanogaster* possesses 152 muscle groups in the imago, as well as 54 in the larva (Bothe & Baylies, 2016). Each muscle is adapted to perform a specialized function, such as the extremely ordered indirect flight muscle (IFM) which is designed so as to enable the rapid oscillatory contractions needed to sustain flight. The marked phenotypic differences among these muscle types begs a molecular explanation. Alternative splicing is known to contribute to muscle type development and function with about 80% of sarcomere proteins being differentially expressed or spliced in Drosophila muscle (Nikonova et al., 2020). One such protein is Zasp52, a scaffolder, which contains numerous alternatively spliced exons generating a variety of isoforms.

All metazoan muscles share considerable structural homology (Steinmetz et al., 2012). They come in two types: striated, which appear striped given the presence of sarcomeres, and smooth, which do not possess sarcomeres. The sarcomere, a cylindrical structure, is the fundamental contractile unit of striated muscle and is bordered on either side by a dense circular structure called the Z-disc. Sarcomeres are arranged end-to-end in long arrays called myofibrils. Thin filaments composed of actin are anchored at and extend perpendicularly from the Z-disc into

neighbouring sarcomeres, terminating at the H-zone (the region halfway between two Z-discs with no thin filaments). Thick filaments composed of muscle myosin are centred at the M-line (found at the centre of the H-zone) and interdigitate with thin filaments in a hexagonal lattice. The mechanism of sarcomere contraction is explained by the sliding filament theory in which thick filaments pull upon thin filaments in an ATP-dependent manner, bringing the Z-discs closer together. The simultaneous contraction of tandem sarcomeres comprising a myofibril is what leads to large-scale muscular contraction (Krans, 2010). The Z-disc is crucial for maintaining mechanical stability of the muscle and contains numerous proteins including Zasp52 which interacts with the thin filament cross-linker alpha-actinin (Liao et al., 2016) and actin (Liao et al., 2020) in Drosophila.

Zasp52, part of the three-membered Drosophila Alp/Enigma protein family along with Zasp66 and Zasp67, is crucial for maintaining structure at the Z-disc. It localizes to the Z-disc in all muscle types of *Drosophila melanogaster* (Katzemich et al., 2011) and is required for the assembly and maintenance of IFM sarcomeres (Katzemich et al., 2013; Liao et al., 2016). Developmentally, Zasp52 appears in the embryo first at myotendinous junctions and also at Z-bodies - clusters which later coalesce to form Z-discs (Katzemich et al., 2013). Zasp52 binds actin via its N-terminal PDZ domain plus a long C-terminal extension (Liao et al., 2020), and α-actinin via a region encompassing the PDZ domain plus a short C-terminal extension (Liao et al., 2016). In addition to the PDZ and Zasp motif (ZM) domain, Zasp52 contains four LIM domains which interact with the ZM domain resulting in auto-oligomerization; this mechanism is believed to drive radial growth of the Z-disc as well as pathological aggregate formation (González-Morales et al., 2019). Its primary human ortholog LDB3/ZASP is implicated in muscular dystrophies which are characterized by progressive adult-onset distal myofibrillar myopathy and sometimes cardiomyopathy (Griggs, et al., 2007).

Zasp52 is alternatively spliced into twenty-two different isoforms (according to FlyBase release FB2025_02, used throughout this paper), which leads to a variety of different domain and inter-domain combinations. The inter-domain linker regions connecting Zasp52's structured domains (i.e., PDZ, ZM, and LIM domains) are less characterized but play an important role in protein function (Fisher & Schöck, 2022). Isoforms containing the first and second LIM domains contain a linker region between the two which can vary greatly in size. Encoded by several exons, this linker region may contain exon 15 which undergoes alternative 5' splice site selection generating five exonic variants (15a-e) ranging from 130 nucleotides (15a) to 4429 nucleotides (15e) in length (Fig. 1A). The last 29 nucleotides of exon 15 contribute to the second LIM domain, but the remainder encodes the linker. When exon 15e is included, it constitutes the majority of the entire protein, encoding 1475 amino acids which total 160 kDa. In the canonical and longest isoform Zasp52-PF, the entire protein is 2194 amino acids long and the linker region between LIM1 and LIM2 is 1686 amino acids long. Exon 15e is referred to variously by other sources: as exon 9 in Flybase, exon 16c in Katzemich et al., 2011, and exon 18/19 in Benna et al., 2009; protein isoforms containing exon 15e were previously also referred to as Z(210) (Chechenova et al., 2013).

Though not much is known about this linker region between LIM1 and LIM2, its predominant expression in IFM and unusually large length prompted us to investigate it. We were curious to see how deleting only exon 15e while retaining all conserved domains would affect muscle structure and function. This linker was found to be highly disordered; intrinsically disordered regions (IDRs) have mostly been analyzed biochemically, with only limited data on their *in vivo* function in model organisms (Jensen et al., 2025). Flight ability was impaired and myofibrils displayed a variety of phenotypes which were all indicative of a loss of thin filament anchoring at the Z-disc. Most phenotypes exhibited an age-related increase in severity. Put together, these data demonstrate a crucial role of this large IDR in maintaining sarcomere integrity by stabilizing thin filaments at the Z-disc in IFM.

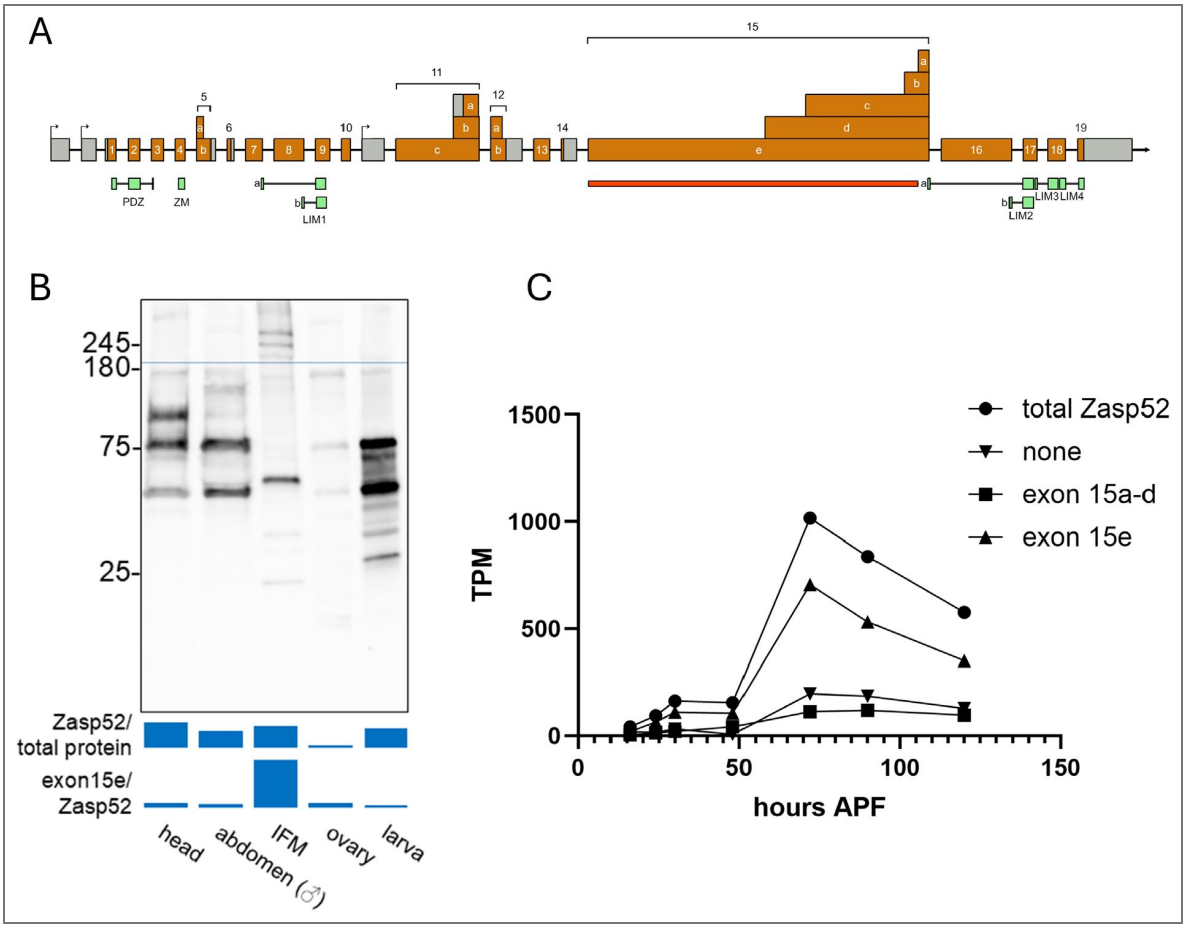

Figure 1. exon 15e-containing isoforms are expressed in a specific spatiotemporal manner

(A) A schematic of the Zasp52 locus. Exons are drawn to scale, introns are not. Coding exons are orange and untranslated regions in grey. Alternative start sites are also indicated. Below in green are mappings of structured domains according to SMART (Letunic & Bork, 2018); and also Katzemich et al, 2011 which defined LIM1 and LIM2 variants. The deletion in *ex15e* mutants is indicated in red. **(B)** Western blot using five different tissue extracts from control flies probed with a Zasp52 full-length antibody. Relative amounts of Zasp52 content as measured in each lane, over the total protein content as measured using the TGX Stain-free gel method, are quantified below for each tissue. Exon 15e content as measured using the protein content above the dotted blue line for each lane, over Zasp52 content is quantified below that. Molecular weights appear higher, perhaps due to retardation caused by non-specific interactions with the gel matrix, as also seen in Watts et al., 2017, Fig. S1. **(C)** RNA-seq data from Spletter et al., 2018 of IFM tissue across various timepoints after puparium formation; the last timepoint is of adults one day after eclosion. Gene expression levels in transcripts per million (TPM) are shown for Zasp52 isoforms classified according to their splicing of exon 15.

Results

exon 15e-containing isoforms are expressed in a specific spatiotemporal manner

Western blotting using a polyclonal antibody capable of detecting all Zasp52 splice variants (hereinafter referred to as the Zasp52 full-length antibody, Jani & Schöck, 2007) was used to analyze the presence of Zasp52 in IFM, ovaries, whole larvae, heads, and whole male abdomens (Fig. 1B). IFM contains the second most Zasp52 protein of any isoform relative to total protein content compared to the other tissues analyzed and is the only tissue that significantly contains exon 15e-containing isoforms relative to total Zasp52 content. This agrees with previous studies (Chechenova et al., 2013, Benna et al., 2009) which found no higher weight isoforms in larvae, and with transcriptomics data. Whole organism RNA-seq data from the ENCODE project (Duff et al., 2015) reveals very little expression of exon 15e in all developmental stages up until four days past the white prepupal stage (Fig. S1). To verify that this is indeed a phenomenon of exon 15e inclusion and not merely Zasp52 expression, one can look at the surrounding exons which do not follow the same pattern as exon 15e. To gain a more precise perspective on IFM expression of exon 15e, we turned to an RNA-seq dataset from Spletter et al., 2018 which looked at total RNA content of IFM at various developmental time points (Fig. 1C). Expression of all Zasp52 transcripts in IFM surges from 48 to 72 h after puparium formation (APF), with most of these transcripts containing exon 15e, as opposed to including exon15 a-d only or no exon 15 at all.

We used various software to predict the level of disorder across Zasp52-PF (Fig. S2A). All identified the linker region between LIM1 and LIM2 as an intrinsically disordered region (IDR) to various degrees, although some regions within it appear more ordered. The actin-binding motif identified by Ashour et al., 2023 within exon 15e is predicted to be more structured than the surrounding regions. No significant sequence similarity was found when aligning Zasp52's linker region to human or other *Drosophila melanogaster* ALP/Enigma protein family members. We then compared the lengths of the linker regions between LIM1 and LIM2 in all insect species possessing a Zasp52 ortholog as defined by NCBI's Eukaryotic Genome Annotation Pipeline (Fig. S2B). Drosophilids generally have a longer linker than their taxonomical neighbours. Mayflies, dragonflies, and damselflies, which use direct flight muscle, have notably short linkers. Since linear sequence often does not fully describe an IDR's function, we analyzed linear clustering or mixing of different residue types using NARDINI (Cohan et al., 2022). The z-score matrix of the linker region between LIM1 and LIM2 in Zasp52-PF showed a strong clustering/segregation of polar residues (μ), as well as alanine (A) and proline (P), and hydrophobic residues (h) (Fig. S2C). The z-score matrix of exon 15e alone displayed much of the same clustering, except with additional strong clustering of acidic residues (-) with respect to other residue classes (Fig. S2C'). This implies that the additional exons in the linker region dilute or mask the strong clustering of acidic residues in exon 15e alone. We attempted to compare z-score matrices across various arthropod species but were unable to detect any meaningful correlation indicating that the binary patterns uncovered by NARDINI do not reveal taxonomical differences in exon 15e composition.

A CRISPR deletion of exon 15e displays flight defects

To further investigate the function of exon 15e, we generated a CRISPR deletion spanning five intronic nucleotides five prime to exon 15e up to 149 nucleotides before the 3' end of exon 15e (Fig. 1A). In total, 4285 nucleotides totaling 156 kDa were deleted. Thus, our mutants would affect all isoforms containing exons 15b-e. The deletion endpoints were sequenced to confirm effective CRISPR knockout. To confirm that our deletion worked and spliced as intended, we performed Western blots using the Zasp52 full-length antibody to compare our deletion with a control and the MiMIC line MI00979 (Venken et al., 2011) which truncates everything C-terminal to and including exon 15e (Fig. 2A). The largest protein that could possibly be present in our mutant would be 136 kDa (Zasp52-PI). Our deletion was devoid of all higher molecular weight isoforms containing exon 15e which were present in the control as expected. Our deletion also

contained several isoforms which were heavier than the highest molecular weight isoforms of MI00979 which were also not present in control, suggesting that these are novel products containing the C-terminal LIM domains. To confirm that this was indeed the case, i.e., that the three C-terminal LIM domains were retained, we raised an antibody against them and performed a Western blot (Fig. 2A'). Our CRISPR deletion retained these LIM domains as expected. We refer to this CRISPR mutant as *ex15e*.

We wanted to see how *ex15e* affected the locomotory abilities of the fly. Since larvae do not express exon 15e, we do not expect them to be affected by our deletion. Therefore, we performed a larval crawling assay as a negative control to confirm that *ex15e* larval muscles were unaffected (Fig. 2B). As predicted, control and *ex15e* larvae demonstrated no differences in crawling ability. Next, we wanted to see how flight would be affected, given that exon 15e is present primarily in the adult IFM. *ex15e* flies of all age categories had impaired flight ability compared to control with a severe deterioration at three weeks of age (Fig. 2C). To ensure that no secondary-site mutations were affecting our mutant phenotypes, we performed a simple binary flight assay using the heterozygous *ex15e* deletion over a Zasp52 deficiency (Fig. S3A).

This impairment in flight could stem from a variety of causes, given the multimodal functionality of Zasp52. We decided to first look at gross muscle morphology before zooming in on our investigation. Thorax bisections revealed no noticeable difference in the IFMs of *ex15e* and control flies (Fig. S3B, C). Since Zasp52 was known to be involved in integrin interactions (Jani & Schöck, 2007) and junctional components (Ashour et al., 2023), we inspected the myotendinous junctions of IFM, which are called modified terminal Z-discs (MTZ), in three-week-old flies (Fig. S3D-G"). βPS integrin localization appeared unaffected in *ex15e*; this agrees with integrins being upstream of Zasp52 (Jani & Schöck, 2007). However, the MTZ appeared disrupted and malformed, lacking the organized structure seen in controls. Furthermore, we also noticed myofibril defects which prompted us to further investigate IFM at the myofibrillar level.

ex15e mutant IFM phenotypes: bending at the Z-disc and thin filament intrusion into the H-zone

IFM tissue was analyzed by confocal microscopy with several phenotypes being observed. First, myofibrils in *ex15e* mutants were often found to be bent at the Z-disc (Fig. 3A-C). In control flies, sarcomeres across different age groups typically displayed the same proportion of degree of bentness. In *ex15e*, the proportion of bent sarcomeres increased with age, as well as the degree of bending, compared to control flies. Force-induced bending results in a sarcomere whose inner curve is bowed, much like a hose with a kink. The bending in *ex15e* appears to be a result of the improper anchoring of thin filaments which leads to a shear type angle shift in the sarcomere at the Z-disc. Bending was found exclusively at the Z-disc and not the M-line in all muscle analyzed.

Another phenotype observed in *ex15e* was the presence of a dense band of actin staining at the H-zone, where normally there would be no actin staining (Fig. 3D-G). Control flies have very few sarcomeres with this phenotype at all ages; *ex15e* are similar to control at one day of age but begin to accumulate a large number of these abnormal sarcomeres with time. At three weeks of age, a large proportion of sarcomeres have actin at the H-zone. Usually, groups of myofibrils in the same area would exhibit this phenotype rather than these abnormal myofibrils being randomly dispersed among the normal ones. This dense band of actin suggested that thin filaments were overlapping at the M-line. This could be a result of hypercontraction, where thin filaments are brought so close together that they overlap. However, the protocol used for these preparations includes a relaxing solution containing ATP, which induces cross-bridge detachment resulting in the adoption of a relaxed conformation. To see if these abnormal sarcomeres with actin in the H-zone were indeed contracted, we measured their length and compared them to normal sarcomeres from the same sample in three-week-old flies (Fig. 3G). Sarcomeres with actin in the H-zone had a smaller length than those without indicating that they were indeed contracted. Muscle decontraction relies on the elastic nature of the sarcomere to restore it to a relaxed

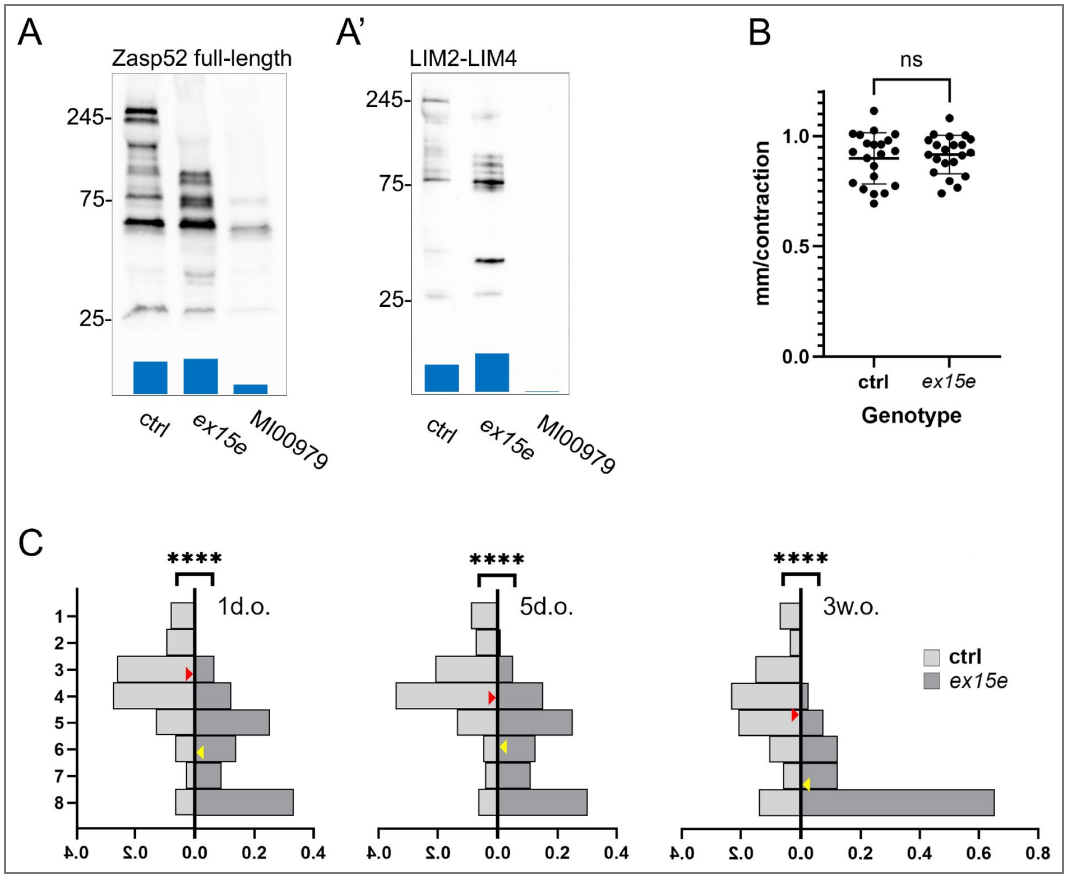

Figure 2. A CRISPR deletion of exon 15e displays flight defects

Western blots using either the Zasp52 full-length antibody **(A)** or antibody against LIM2-LIM4 **(A')** of either w^{1118} (ctrl hereinafter), *ex15e*, or the MiMIC line MI00979 whole flies. Relative amounts of Zasp52 content as measured in each lane, over the total protein content, are quantified below for each genotype. **(B)** Larval crawling assay of either ctrl (n=21) or *ex15e* (n=21) third instar larvae showing no significant difference between the two (Unpaired t-test with Welch's correction; p=0.6006). **(C)** Flight assays of ctrl vs *ex15e* flies of three different age categories: one-day-old (ctrl n=138 flies, *ex15e* n=123), five-days-old (ctrl n=125, *ex15e* n=119), and three-weeks-old (ctrl n=86, *ex15e* n=81). The y-axis indicates flight strength: flies were released into a tube and those that landed in the top segment (y=1) had the strongest flight strength while those that landed in the bottom dish (y=8) had the weakest. The x-axis indicates the proportion of flies that landed in that segment. Red arrows indicate the average position landed in control flies, yellow arrows are for *ex15e* flies. Difference in flight ability was statistically significant for all age categories (Fisher's exact test; p<0.0001).

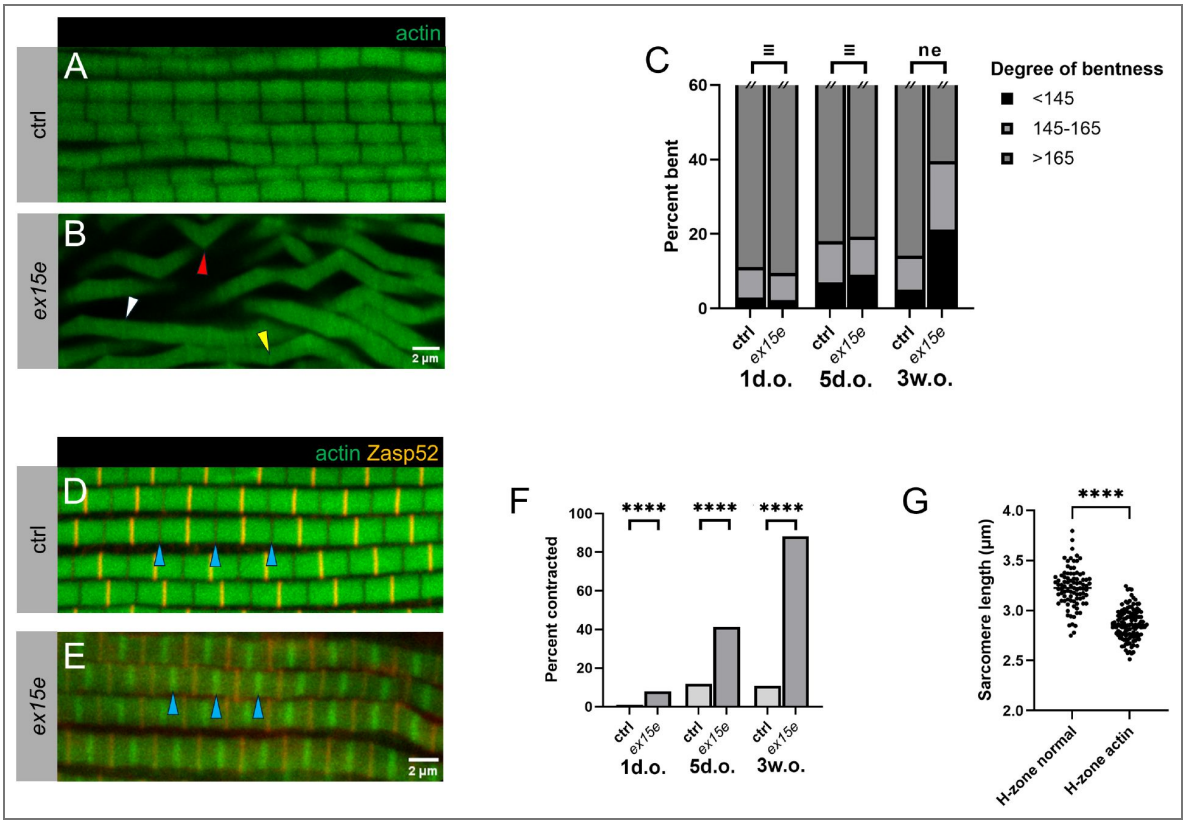

Figure 3. *ex15e* mutant IFM phenotypes: bending at the Z-disc and thin filament intrusion into the H-zone

(A-C) Analysis of bent sarcomere phenotype. Actin is visualized by phalloidin in green. Control myofibrils **(A)** appear straight while *ex15e* **(B)** myofibrils contain a range of bending (representative three-week-old myofibrils shown). Red arrow indicates a representative sarcomere with a bend of <145°, yellow indicates 145-165°, and white >165°. Bend angles were statistically equivalent (≡) between ctrl and *ex15e* in one-day-olds and five-day-olds, but not equivalent (ne) in three-week-olds, where *ex15e* displayed greater bentness **(C)**. Sample sizes: one-day-old (ctrl n=1242 sarcomeres, *ex15e* n=1851), five-days-old (ctrl n=1192, *ex15e* n=946), and three-weeks-old (ctrl n=1768, *ex15e* n=1125) (Two One-Sided Test (TOST) with ±4.5° equivalence margin, α=0.05; 1d.o. t_L=12.95, t_U=-12.07; 5d.o. t_L=6.03, t_U=-8.01; 3w.o. t_L=-6.34, t_U=-20.63). **(D-F)** Sarcomeres also exhibited actin in the H-zone phenotype (representative three-week-old myofibrils shown). Control **(D)** myofibrils display normal H-zones without actin with M-lines/H-zones indicated by blue arrows. *ex15e* **(E)** myofibrils display actin accumulation at the H-zone; arrows indicate same as above. Actin is visualized by phalloidin in green and Z-discs are identified by the full-length Zasp52 antibody in red. These sarcomeres with H-zone actin, which appear hypercontracted, are significantly overrepresented in *ex15e* compared to control across all age categories **(F)**. Sample size were as follows: one-day-old (ctrl n=3255 sarcomeres, *ex15e* n=4056), five-days-old (ctrl n=3221, *ex15e* n=2677), and three-weeks-old (ctrl n=5394, *ex15e* n=4720 (Fisher's exact test; p<0.0001). To confirm that H-zone actin sarcomeres were indeed contracted, the Z-to Z-disc length was measured in *ex15e* three-week-old flies of both sarcomeres with a bare H-zone (H-zone normal, n=89 sarcomeres) and those with actin in the H-zone (H-zone actin, n=117) (**G**). H-zone actin sarcomeres were significantly smaller (Unpaired t-test with Welch's correction; p<0.0001).

conformation once myosin heads detach from the thin filaments. This requires stable Z-discs and myofilament attachments, the lack of which may be the cause of a permanent hypercontracted state in *ex15e*.

To gain a better understanding of this phenomenon, we performed transmission electron microscopy (TEM) of myofibrils and noticed phenotypes that concurred with our immunofluorescence confocal images (Fig. 4). Z-discs were highly disrupted and contained many holes and broken regions. M-lines were also affected in a similar manner. Gaps between filaments were abundant and in general appeared more disorganized than control. Filaments were often frayed at the edges of the sarcomeres.

Most *ex15e* defects are restored by rescue constructs

To determine if the phenotypes are truly due to the IDR or are caused by an altered isoform composition, we wanted to see if the phenotypes of *ex15e* could be rescued. First, we expressed either UAS-Zasp52-PF or UAS-Zasp52-PR using a UH3-GAL4 driver in a homozygous *ex15e* background and examined three-week-old flies (Fig. 5B-H). Zasp52-PF is the canonical full-length Zasp52 isoform which contains exon 15e, while Zasp52-PR contains all structured domains but not exon 15e (Fig. 5A). The degree of bending in Zasp52-PR rescue sarcomeres was statistically equivalent to that of *ex15e* mutants, while that of Zasp52-PF rescues was equivalent to control flies, indicating that Zasp52-PF but not Zasp52-PR can rescue this phenotype (Fig. 5F). The proportion of H-zone actin (i.e., hypercontracted) sarcomeres was not significantly different between *ex15e* and Zasp52-PR rescues as expected. Interestingly, no hypercontracted sarcomeres were observed upon re-expression of Zasp52-PF again indicating a successful rescue (Fig. 5G). Finally, we tested flight ability and observed a significant increase in flight strength in Zasp52-PF rescues compared to Zasp52-PR rescues, with the latter being not significantly different from *ex15e* (Fig. 5H). Zasp52-PF rescues were still weaker fliers than control flies suggesting a partial rescue of flight ability.

ex15e and actin genetically interact

We next wanted to test for a genetic interaction between exon 15e and Act88F (the actin isoform present in IFM) by analyzing heterozygous *ex15e*, heterozygous $Act88F^{KM88}$ (an amorphic mutant of *Act88F*), and a di-heterozygous combination of both (*ex15e*/+; $Act88F^{KM88}$/+) (Fig. 6). *ex15e*/+ resembled control myofibrils and $Act88F^{KM88}$/+ has mild myofibrillar defects. *ex15e*/+; $Act88F^{KM88}$/+ exhibited supra-additive effects where we often noticed a novel phenotype of very large H-zones. A ratio of twice the thin filament length to the total sarcomere length was computed for all genotypes. Lower values represented sarcomeres whose thin filaments occupied a smaller proportion of the sarcomere and consequently had larger H-zones, whereas a value of one represented the absence of an H-zone. This ratio was not significantly different between control, *ex15e*/+, and $Act88F^{KM88}$/+, but was considerably smaller in di-heterozygotes (Fig. 6E), indicating a strong genetic interaction between Act88F and exon 15e.

FRAP reveals defects in *ex15e* protein dynamics

Given the differences we have thus observed in our mutants, as well as the great length of the IDR, we decided to investigate Zasp52 kinetics in *ex15e* sarcomeres by performing Fluorescence Recovery After Photobleaching (FRAP) (Fig. 7A, C). We expressed GFP-tagged Zasp52-PR (see Fig. 5A) which lacks exon 15e in either a wild-type background as our control (UH3>GFPZasp52-PR), or in an *ex15e* background (*ex15e*; UH3>GFPZasp52-PR). We demonstrate in Fig. 5 that Zasp52-PR cannot rescue *ex15e*. One-day-old IFM Z-discs were photobleached and recovery of fluorescence was monitored. Fluorescence recovery in the *ex15e* background was to a significantly higher level indicating a larger mobile fraction (Fig. 7B). A greater mobile fraction in our mutant background signifies that exon 15e is required to hold Zasp52 in place at the Z-disc, either by fastening itself, or keeping other molecules in place thereby contributing to overall Z-disc stability.

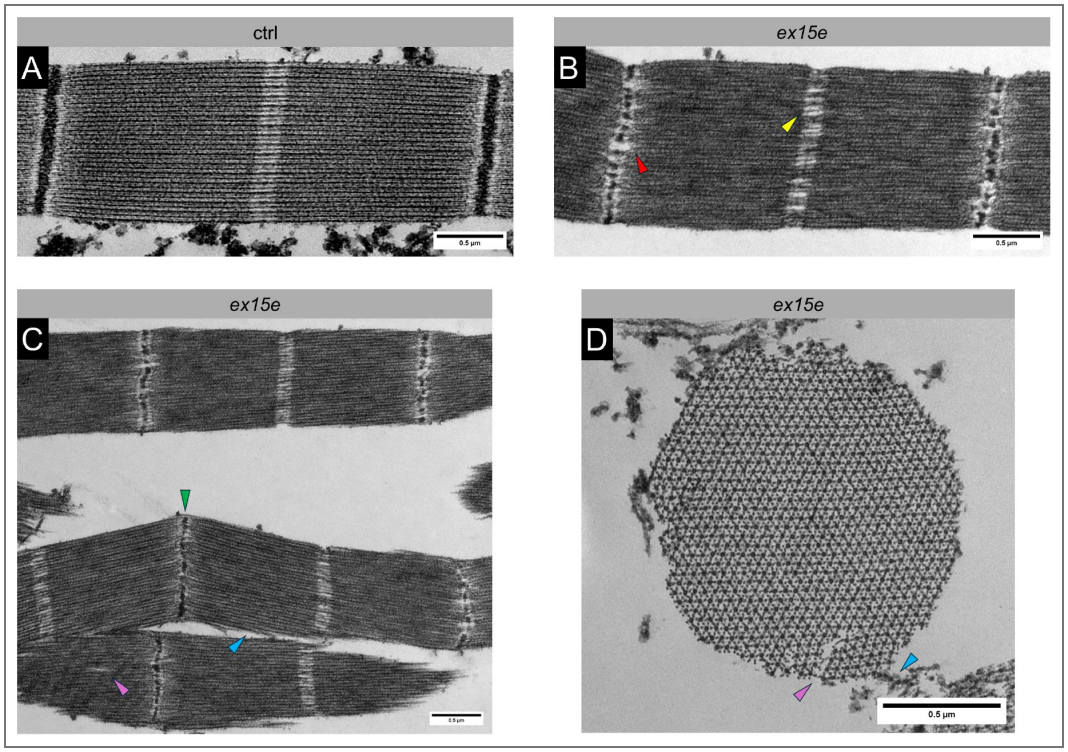

Figure 4. TEM reveals defects in mutant sarcomere ultrastructure

TEM images reveal similar phenotypes as immunofluorescent ones (three-week-old shown). Control **(A)** sarcomeres are very structured and even. Longitudinal sections of *ex15e* **(B**,**C)** display broken Z-discs (red arrow), broken M-lines (yellow), bending at the Z-discs (green), splits in filaments (purple), and fraying peripheral filaments (blue). Transverse sections of *ex15e* **(D)** also display some of these abnormalities.

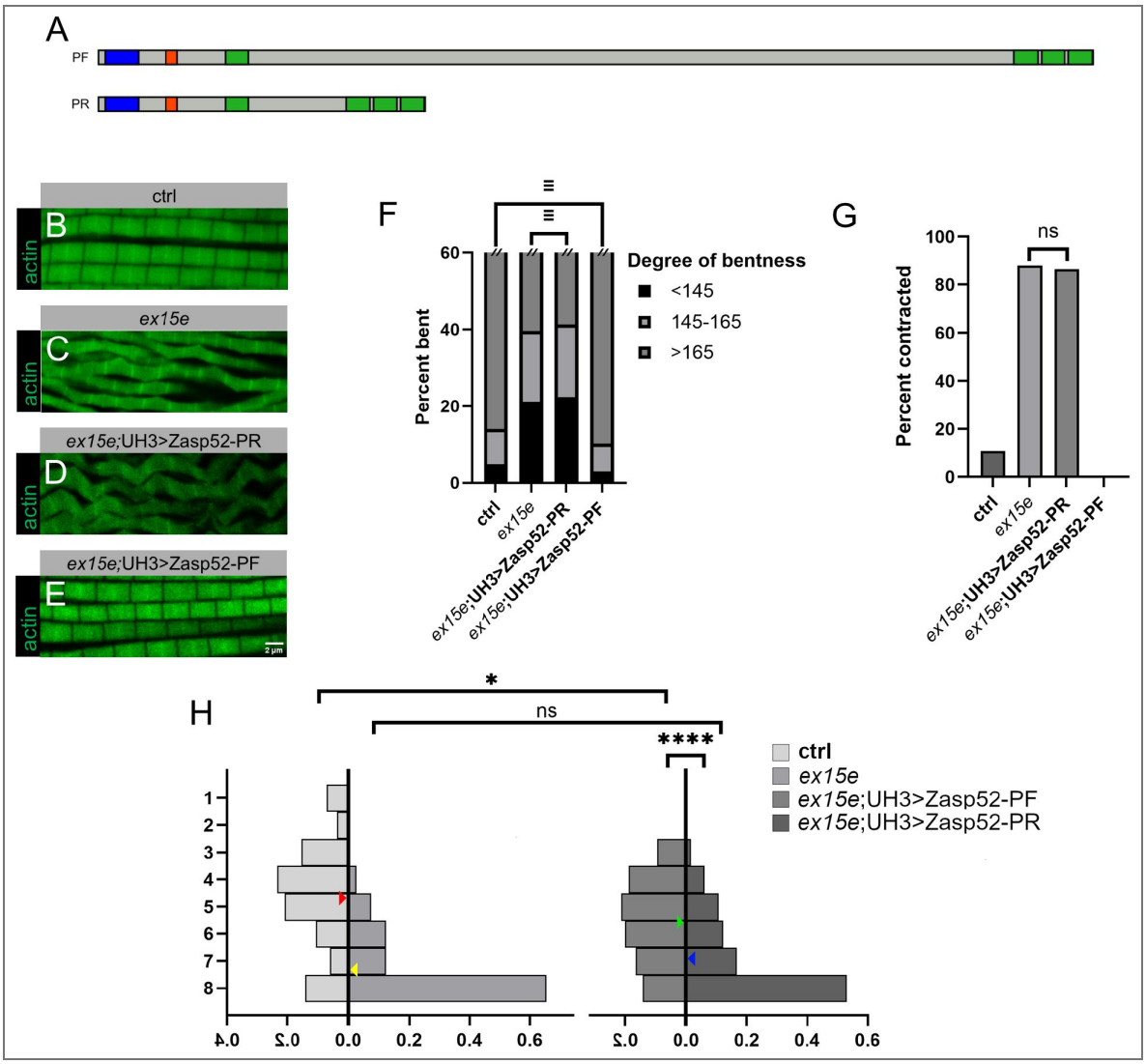

Figure 5. Certain *ex15e* defects are restored by rescue constructs

Zasp52-PF or Zasp52-PR was heterozygously overexpressed with a UH3-GAL4 driver over a homozygous *ex15e* background in a rescue attempt. In this figure, all myofibrils had actin visualized with phalloidin in green, all experiments were done at three weeks of age, and ctrl and *ex15e* data are same as previous. **(A)** Schematic showing Zasp52-PF which is the canonical full-length isoform, and Zasp52-PR which contains all structured domains but lacks exon 15e. PDZ domain (blue), ZM (red), LIM domains (green). **(B-E)** Myofibrils display bending, Z-disc disruption, and overall myofibrillar disorganization in Zasp52-PR overexpressions **(D)**, while Zasp52-PF overexpression **(E)** appears similar to ctrl **(B)**. Bend angles were equivalent (≡) between *ex15e* and *ex15e*; UH3>Zasp52-PR, and between ctrl and *ex15e*; UH3>Zasp52-PF **(F)**. Sample sizes: *ex15e*; UH3>Zasp52-PR n=2049 sarcomeres, *ex15e*; UH3>Zasp52-PF n=2221. (Two One-Sided Test (TOST) with ±4.5° equivalence margin, α=0.05; *ex15e-ex15e*; UH3>Zasp52-PR t_L=1.92, t_U=-10.16; ctrl-*ex15e*; UH3>Zasp52-PF t_L=17.65, t_U=-8.51). The proportion of sarcomeres that were contracted (i.e., actin in H-zone) was not significantly different between *ex15e* and *ex15e-ex15e*; UH3>Zasp52-PR, whereas no such sarcomeres were found in *ex15e*; UH3>Zasp52-PF **(G)**. Sample sizes: *ex15e*; UH3>Zasp52-PR n=2843 sarcomeres, *ex15e*; UH3>Zasp52-PF n=2480. (Fisher's exact test p=0.0521). **(H)** Flight ability between *ex15e*; UH3>Zasp52-PR (n=66) and *ex15e*; UH3>Zasp52-PF (n=85) was significantly improved, with *ex15e*; UH3>Zasp52-PR showing no significant difference from *ex15e* but *ex15e*; UH3>Zasp52-PF showing significant difference from ctrl. The y-axis indicates flight strength: flies were released into a tube and those that landed in the top segment (y=1) had the strongest flight strength while those that landed in the bottom dish (y=8) had the weakest. The x-axis indicates the proportion of flies that landed in that segment. Red arrows indicate the average position landed in control flies, yellow are *ex15e*, green are *ex15e*; UH3>Zasp52-PR, and blue are *ex15e*; UH3>Zasp52-PF. (Fisher's exact test; *ex15e*; UH3>Zasp52-PR-*ex15e*; UH3>Zasp52-PF p<0.0001; *ex15e-ex15e*; UH3>Zasp52-PR p=0.2668; ctrl-*ex15e*; UH3>Zasp52-PF p=0.0129).

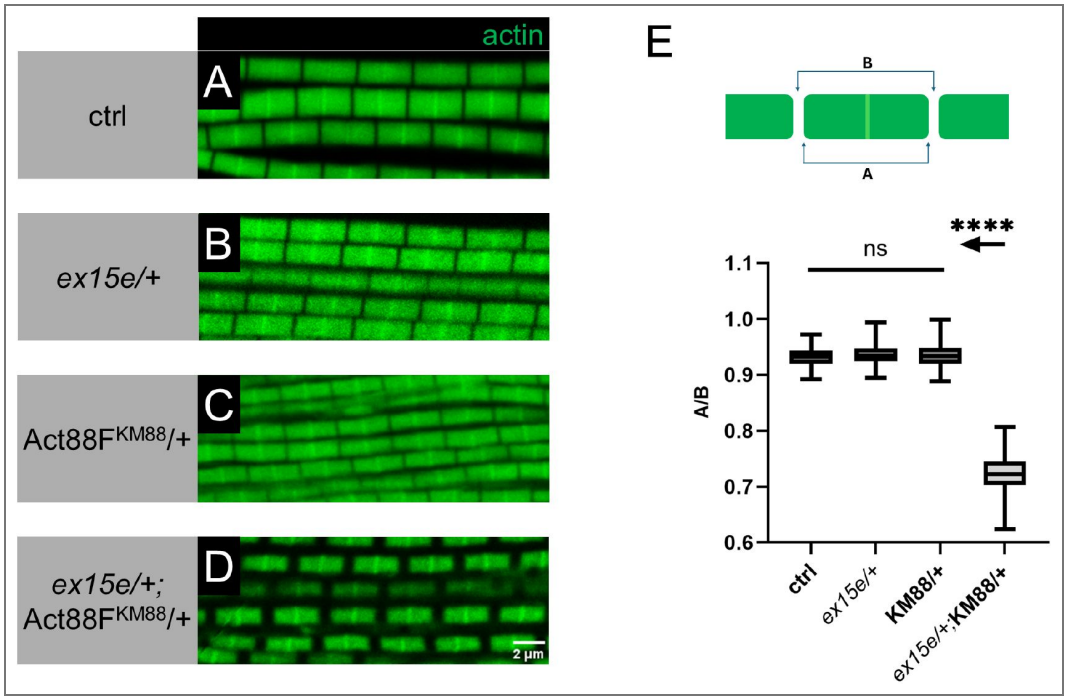

Figure 6. Large H-zones demonstrate a genetic interaction between exon 15e and Act88F

(A-D) Myofibrils of one-day-old flies of various genotypes. Actin was visualized with phalloidin in green. Control and heterozygous *ex15e* myofibrils appear indifferentiable; heterozygous *Act88F*^{KM88} are slightly disrupted with fraying and slight narrowing. Representative *ex15e*/+; *Act88F*^{KM88}/+ myofibrils with large H-zones are shown. The ratio of twice the thin filament length denoted distance "A" to the corresponding sarcomere's length denoted as "B" for all four genotypes is quantified in **(E)**. A schematic illustrates the measurement of these distances. Sample sizes were as follows: ctrl *n*=119 sarcomeres, *ex15e*/+ *n*=122, *Act88F*^{KM88}/+ *n*=119, *ex15e*/+; *Act88F*^{KM88}/+ *n*=119. The ratio A/B represents the proportion of the sarcomere length occupied by thin filaments and is inversely correlated with H-zone length; *ex15e*/+; *Act88F*^{KM88}/+ sarcomeres have significantly larger H-zones than all others. All sarcomeres with an *Act88F*^{KM88} allele were radially narrower than control, but a synthetic enhancement could not be concluded from this observation. (Unpaired t-test with Welch's correction; ctrl-*ex15e*/+ p=0.0502; ctrl-*Act88F*^{KM88}/+ p=0.2770; ctrl-*ex15e*/+; *Act88F*^{KM88}/+ p<0.0001; *ex15e*/+-*Act88F*^{KM88} p=0.4938; *ex15e*/+-*ex15e*/+; *Act88F*^{KM88} p<0.0001; *Act88F*^{KM88}/+-*ex15e*/+; *Act88F*^{KM88} p<0.0001).

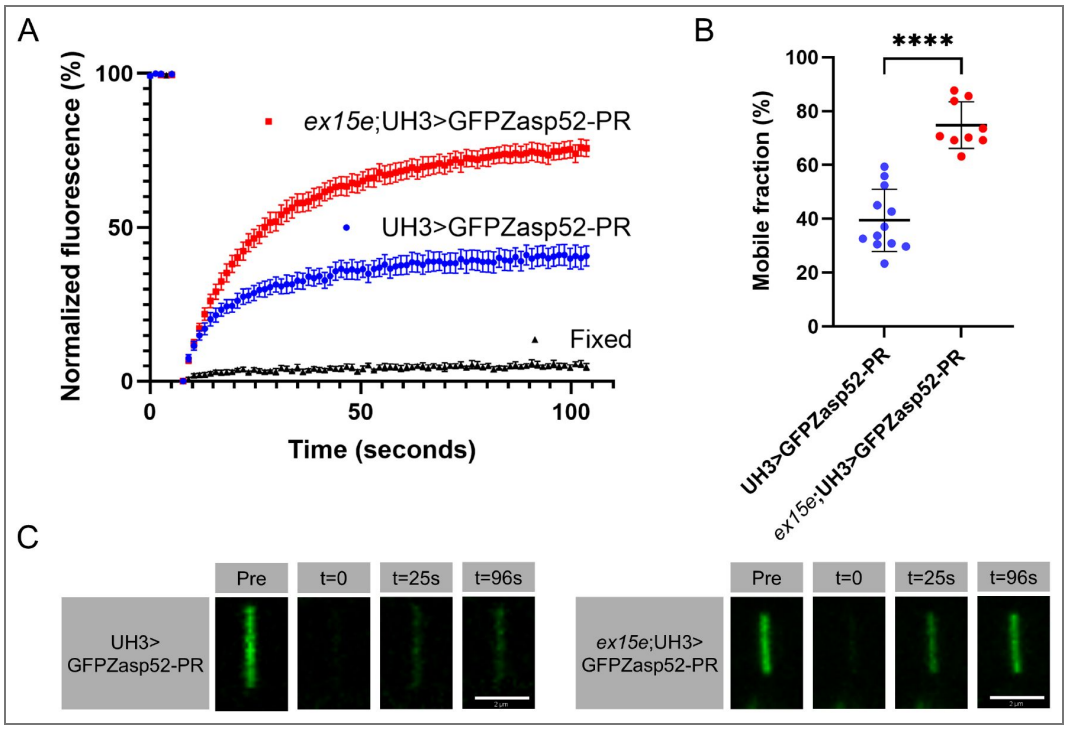

Figure 7. FRAP reveals defects in *ex15e* protein dynamics

FRAP experiments visualizing recovery of GFPZasp52-PR were performed on one-day-old female IFM Z-discs either in our mutant background (*ex15e*;UH3>GFPZasp52-PR, *n*=9 flies) or wild-type background which served as a control (UH3>GFPZasp52-PR, *n*=12) **(A)**. Control UH3>GFPZasp52-PR Z-discs fixed with 4% paraformaldehyde for 10 minutes (labelled "Fixed", *n*=7) displayed no recovery as expected. Plateaus of fitted curves were significantly different, with a greater mobile fraction in the mutant background (Unpaired t-test with Welch's correction; $p<0.0001$) **(B)**. Representative snapshots of bleached Z-disc recovery illustrate this difference between genotypes **(C)**.

Most *ex15e* defects are rescued by immobilization

On a different note, we noticed that virtually all the *ex15e* phenotypes worsened with age, which suggests that use might contribute to deterioration. We therefore decided to prevent flies from using their IFMs by immobilizing them (Fig. 8). Flies were reared until three weeks of age in between glass plates separated by 1.5 mm spacers which prevented them from flying or even attempting to fly. The degree of bending in immobilized flies was equivalent to that of control flies (Fig. 8D). The proportion of hypercontracted sarcomeres was also not significantly different between immobilized and control flies (Fig. 8E). Intriguingly, even flight ability was restored in immobilized flies compared to age-matched controls with no significant difference between the two (Fig. 8F). These results suggest successful rescue by preventing IFM use via immobilization.

Discussion

Traditionally, IDRs were associated with the concept of amorphousness, finding themselves in transient structures such as condensates and membraneless organelles. As our understanding of disordered proteins has changed, their role in more disparate contexts has become increasingly appreciated, revealing them as modular hubs, flexible scaffolds, and more (Cortese et al., 2008). Furthermore, their role in disease has spurned great interest in their myriad functions. In this study, we demonstrate the role of an exceptionally large disordered region, Zasp52's exon 15e, in maintaining stability and integrity in a highly rigid and force-bearing structure – the Z-disc.

First, we showed that the expression of exon 15e is spatiotemporally regulated. Being confined to the adult IFM suggests that exon 15e's function is uniquely required for the rapid oscillatory contractions in indirect flight. Supporting this is the fact that the linker region containing exon 15e is generally much longer in Drosophilids, and rather short in insects using direct flight. Although this linker region is predicted by multiple software programs to be disordered, within it are regions of greater order, one of which corresponds to a putative actin-binding motif (Ashour et al., 2023). This arrangement exists in other proteins such as Cno in Drosophila, where higher-ordered actin-binding regions are embedded in a large IDR (Jensen et al., 2025). Furthermore, a synthetic enhancement between *ex15e* and $Act88F^{KM88}$ heterozygotes indicates that exon 15e and actin genetically interact. There may be other important short linear motifs (SLiMs) contained within the linker region which serve as interacting sites with other sarcomere proteins. Indeed, multiple sequence alignment of the linker regions of various insects reveals several conserved motifs of unknown function. The presence of an actin-binding motif that may strengthen thin filament anchoring to the Z-disc would be in line with the phenotypes we observed in *ex15e*. Bending at the Z-disc is indicative of a loss of thin filament anchoring and stability at the Z-disc, allowing them to shift out of alignment. Normal sarcomeres bent due to force would exhibit a kinked-hose appearance, where the inner edge is sharply bent and the outer one bowed. This was occasionally observed in controls, whereas *ex15e* bends were always shifted uniformly. Actin in the H-zone is also indicative of loss of stable thin-filament anchoring. During preparation, IFMs are incubated overnight in skinning solution during which they enter a state of rigor. After washing them with an ATP-containing relaxing solution, the myosin heads detach from the thin filaments and the supple nature of the sarcomere which provides it with elastic recoil, causes it to resume a relaxed conformation. However, when thin filaments are weakly anchored at the Z-discs, the natural tension contained within the sarcomere is reduced and thus it will not "bounce back" into a relaxed conformation, resulting in a hypercontracted state which manifests as actin continuing to reside in the H-zone. Cheerio, a Drosophila filamin, was shown to stably attach actin thin filaments at the Z-disc and induces a similar actin incorporation into the H-zone when mutated (González-Morales et al., 2017). Thus, we also demonstrate the importance of Z-disc integrity in allowing sarcomeres to return to their relaxed state in rapidly contracting asynchronous IFM. Accordingly, synchronous muscles do not have such regularly structured Z-discs, and do not require Zasp52's exon 15e. Indeed, exon 15e is absent in larval and other muscle types. We therefore propose that exon 15e is uniquely required to stabilize rapidly contracting asynchronous IFM.

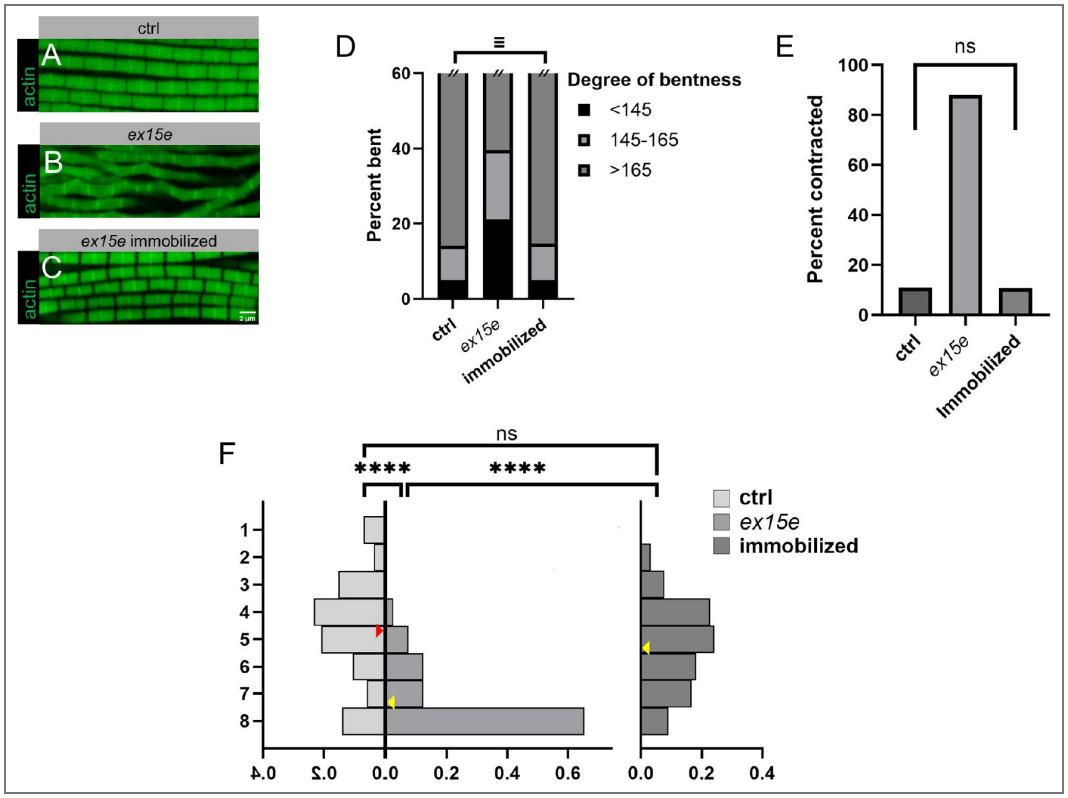

Figure 8. Certain *ex15e* defects are rescued by immobilization

Rescues were attempted by immobilizing flies thereby preventing IFM use. *ex15e* myofibrils in flies that were immobilized **(C)** resembled those of ctrl **(A)**. Bend angles were equivalent between ctrl and *ex15e* immobilized flies (n=2119) **(D)**. (Two One-Sided Test (TOST) with ±4.5° equivalence margin, α=0.05; t_L=15.36, t_U=-12.00). The proportion of sarcomeres that were contracted was not significantly different between ctrl and immobilized flies (n=2246) **(E)**. (Fisher's exact test p=0.2026). Flight ability was rescued with immobilized flies (n=67 flies) having no significant flight defect compared to control (n=86) but being significantly improved from their non-immobilized counterparts (n=81) **(F)**. (Fisher's exact test; ctrl-immobilized p=0.0640; ctrl-*ex15e* and *ex15e*-immobilized p<0.0001).

The orthologous human ALP/Enigma family consists of seven members, with LDB3 (ZASP) considered the canonical Zasp52 ortholog. Zasp52 is more precisely a combined ALP/Enigma member; its first LIM domain is sequentially homologous to the single LIM domain of human ALP family members, and its last three LIM domains are homologous to the three Enigma family LIM domains. Though these human proteins do contain disordered linkers connecting their structured domains, they are much shorter than in Drosophila and are not sequentially homologous. The length of Drosophila's linker was likely evolutionarily driven to be large, as we see insects using direct flight to have much shorter linkers. Several pathological mutations have been identified in the linker region between LDB3's PDZ and LIM domains (Vatta et al., 2003), some of which are now known to lie in the actin-binding Zasp motif (ZM) (Lin et al., 2014). Interestingly, LDB3 has three skeletal muscle-specific splice isoforms which are differentially expressed and variably retain/omit exons 9 through 11 of a linker sequence (Lin et al., 2014). The prenatal long (L) isoform contains exons 10 and 11, post-natal long (LΔex10) has only exon 11, and short (S) has only 9. Post-natal LDB3-LΔex10 contains an actin-binding region in its linker region whose function is abolished by the inclusion of exon 10 in LDB3-L. Thus, human Zasp protein linkers also function in actin binding, regulated by developmentally differential expression. Linker regions in several human ALP/Enigma proteins were found to interact with both α-actinin and actin using AlphaFold (Healy & Collins, 2023). The mouse ortholog Cypher also contains tissue-specific splice variants which variably include or omit linker sequences (Huang et al., 2003). Like Zasp52's exon 15e, Cypher is not required for sarcomerogenesis or Z-disc assembly but only maintenance (Zhou et al., 2001).

Our genetic rescues support our hypothesis of exon 15e involvement in stabilizing thin filaments and Z-discs. The rescues also demonstrate that the conserved domains (PDZ, ZM, LIM1-4) are not sufficient for proper Z-disc and thin filament stability in IFM, because Zasp52-PR could not rescue any of the defects. Interestingly, these phenotypes, as well as the flight defects we observed, worsened with age, with defects in one-day-old flies being very minor. This implies that exon 15e is not required developmentally, but rather for the maintenance of sarcomeres which naturally deteriorate with use. We originally hypothesized that since IDRs often lead to protein aggregation and phase separation, exon 15e might drive the formation of Z-bodies, primitive Z-discs which form through the coalescence of diffuse Z-disc proteins including Zasp52. However, given the lack of defects in early Z-discs and the fact that exon 15e expression does not temporally coincide with Z-body formation, we reject this hypothesis. The role of exon 15e in maintenance is supported by immobilization rescues, in which flies were prevented from flying. We opted for a low-ceiling apparatus which we believe would not only prevent flies from flying but discourage them from futilely attempting to utilize their IFM at all. Surprisingly, immobilization restored flight ability to wild type levels. Interestingly, human zaspopathies often manifest late in life, with one study citing onset at 44 to 73 years of age (Selcen & Engel, 2005), much like what we observed in flies. Our data suggest that avoiding strenuous exercise might delay the onset of zaspopathies. Given the maintenance-specific role of exon 15e, but also that as a whole, Zasp52 is indispensable for pupal myofibril development and not just maintenance (Katzemich et al., 2013), Zasp52 appears to have a multifaceted role more complex than previously considered.

Although one-day-old *ex15e* myofibrils are morphologically indistinguishable from controls, we were already able to detect abnormalities in Zasp52 dynamics using FRAP. The presence of recovery suggests that Zasp52 is not immobile as might be assumed for an anchoring protein and does indeed possess kinetics on a sub-minute timeframe. This is supported by significant transcription of the gene, including exon 15e-containing isoforms, into adulthood (Fig. S1). The mobile fraction of Zasp52-PR was significantly increased in a system entirely lacking exon 15e (the PR isoform also lacks exon 15e) indicating a role of exon 15e in retaining Zasp52 at the Z-disc, whether by direct interaction or not. The FRAP data suggest that Zasp52's IDR stabilizes the Z-disc, in line with the electron microscopy data. It suggests that Z-discs can be described as highly solid aggregates in part stabilized by IDRs, on the other end of the spectrum of the transient condensates initially described, thereby further expanding the importance of IDRs for establishing subcellular structures.

Overall, Zasp52 and its isoforms represent a complex toolbox of multifunctional proteins. There has been evidence suggesting that Zasp52 is not required for initial sarcomere assembly in embryos (Rui et al., 2010), important for Z-disc maintenance overall (Rui et al., 2010, Jani & Schöck, 2007, Katzemich et al., 2013), and required for pupal myofibril assembly (Katzemich et al., 2013). The complete picture of Zasp52's varied function is still unclear; however, we have shown that a specific disordered region is required for maintaining IFM and stabilizing the rigidity of Z-discs. The long linker might not only contain protein-interacting regions but also provide the spacing needed for the neighboring structured domains to properly interact with their partners and perform their roles. We have seen in our genetic interaction experiment an inability of thin filaments to properly elongate when Act88F is partially depleted, which further implicates exon 15e not only in Act88F structure but dynamics. Most encouraging is the complete rescue of flight ability through immobilization, which may provide avenues for delaying the onset of human zaspopathies through reducing strenuous exercise.

Materials and Methods

Fly strains and husbandry

Flies were housed at room temperature (22°C) in standard glass vials and food unless indicated otherwise. Immobilized flies were reared in between 3.25×3.25 inch glass plates separated by 1.5 mm spacers; standard food was inserted into the gap. *ex15e* flies were created by Genetivision using CRISPR-mediated homology-directed repair. The gRNA sequences used were TTTGAACTTGA ACTCTAATGTGG for the downstream target and CAGCCTCTCCACCTTTCCGATGG for upstream. The deletion was replaced with a cassette containing a 3xP3DsRed marker flanked by attP landing sites. It was validated by sequencing at the cut sites. The following genotypes were used: *ex15e*, w^{1118} as control in all experiments, Df(2R)BSC427, Act88F^{KM88}, UAS-GFPZasp52-PR, UH3-Gal4, UAS-Zasp52-PF, UAS-Zasp52-PR, Zasp52^{MI00979}. The UAS constructs consist of the respective Zasp52 isoform with an N-terminal ALFA-tag and C-terminal Spot tag. UAS constructs were made by Genscript and injected into w^{1118} by GenomeProlab.

Western blotting

Extracts were prepared by homogenizing ten flies/fly parts in 100 µL RIPA buffer with protease inhibitor plus an equal amount of 2× Laemmli buffer with β-mercaptoethanol. Samples were boiled at 95°C for five minutes and centrifuged at 12,000×rcf for 5 minutes. Supernatant was used for electrophoresis according to standard protocol using a 4-15% BioRad TGX Stain-free gel. Stain-free gels were imaged for total protein content on a BioRad ChemiDoc before protein was transferred onto a nitrocellulose membrane. Standard Western blotting procedures were followed. Primary antibodies used were rabbit anti-Zasp52 full-length (Jani & Schöck, 2007), and a rabbit antibody against the three C-terminal LIM domains of Zasp52 (FEKYLAPTCSKCAGKIKGDCLNAIGKHFHPECFTCGQCGKIFGNRPFFLEDGN AYCEADWNELFTTKCFACGFPVEAGDRWVEALNHNYHSQCFNCTFCKQNLEGQSFYNKGGRPF CKNHAR) made by Genscript; secondary antibody was goat anti-rabbit IgG (H+L) HRP (Invitrogen).

Locomotory assays

For flight assays, flies were reared in vials (unless immobilized) until the desired age, with vials flipped whenever pupae began to appear. Flight assays were conducted in a manner similar to that described in Babcock & Ganetzky, 2014. A tube 22 cm long and 3.2 cm in diameter was placed in a funnel; the bottom of the tube rested 4 cm above the bottom spout of the funnel. The funnel rested in a 60 cm long tube which was 13.5 cm in diameter and covered with TAD Shake & Spray (T-141) on the inside. The bottom of the funnel was 12 cm below the top of the larger tube. The larger tube was divided vertically into seven 8.5 cm segments, with segment 1 being at the top, and segment 7 being at the bottom. A dish containing water was placed below the tube and was considered segment 8. Vials containing flies were dropped down the narrow tube so that they would be ejected into the larger tube and land somewhere along its length. Flies naturally fly

upwards and those with stronger flight would land higher up the tube. Binary flight assays were conducted by releasing flies one at a time and recording whether they could generate any upwards lift. They were raised in the same conditions as above.

For larval crawling assays, third instar larvae of the desired genotype were collected from bottles and assayed according to Post & Paululat, 2018. In brief, videos of larvae on a slightly moistened petri dish were taken. Time segments where larvae were crawling in a straight line continuously for at least ten seconds were analyzed – contractions per distance were measured and recorded.

Muscle preparation and immunofluorescence

Primary antibodies used were rabbit anti-Zasp52 full-length (Jani & Schöck, 2007), rabbit anti-LIM234 (this study), and mouse anti-βPS-integrin (CF.6G11; obtained from Developmental Studies Hybridoma Bank, Brower et al., 1984) at a concentration of 1:200 for all. Secondary antibodies used were Alexa Fluor 647 goat anti-rat (Life Technologies) and Alexa Fluor 488 goat anti-rabbit (Invitrogen) at a concentration of 1:400 for all.

For IFM tissue, a protocol similar to Xiao et al., 2017 was followed (refer to for recipes). Briefly, thoraces with bisected and incubated in Relaxing-Glycerol solution at -20°C overnight. IFM were isolated and fixed in 4% paraformaldehyde for 15 minutes. Fixed IFM were incubated in primary antibodies at 4°C overnight. IFM were incubated in Acti-stain 555 fluorescent phalloidin (Cytoskeleton Inc) and secondary antibodies, at room temperature for one hour. Samples were mounted in Mowiol mounting medium.

For thorax hemisections including MTZ, a scalpel was used to sagittally bisect thoraces. Samples were fixed in 4% paraformaldehyde for 15 minutes and incubated in primary antibodies for one hour at room temperature, and then Acti-stain 555 fluorescent phalloidin and secondary antibodies for one hour at room temperature. Samples were mounted in Mowiol mounting medium using three 0.12 mm spacers.

For TEM, bisected thoraces were treated with 5 mM MOPS, 150 mM KCl, 5 mM EGTA, 5 mM $MgCl_2$, 5 mM ATP, 1% Triton X-100, and protease inhibitor for two hours. then the same solution with 50% glycerol instead of Triton X-100 overnight at 4°C. This was repeated at -20°C. Samples were washed in 5 mM MOPS, 40 mM KCl, 5 mM EGTA, 5 mM $MgCl_2$, 5 mM NaN_3, protease inhibitor, and then fixed in 3% glutaraldehyde and 0.2% tannic acid for two hours. Samples were washed in 20 mM MOPS, 5 mM EGTA, 5 mM $MgCl_2$, 5 mM NaN_3, and then in 100 mM sodium phosphate buffer, 5 mM $MgCl_2$, 5 mM NaN_3. Secondary fixation was performed in 1% osmium tetroxide in the previous sodium phosphate buffer for one hour. Samples were stained in 2% uranyl acetate, washed with water, and underwent a serial dehydration in ethanol. Samples were washed with propylene oxide and serially infiltrated with Mollenhauer Epon-Araldite. After curing in Beem capsules, 70 nm sections were cut and stained in 4% uranyl acetate followed by SATO lead stain.

Fluorescence Recovery After Photobleaching

One-day-old female flies were anaesthetized and their abdomens, wings, and legs removed. Carcasses were pinned down by the head on a silicone dish and immersed in hemolymph-like 3 (HL3) saline (Stewart et al., 1994). Thoraces were sagittally bisected, washed thrice in HL3 saline, and mounted with a 0.12 mm spacer. Imaging was performed immediately using a HC PL APO 63×/1.40 OIL CS2 objective on a Leica SP8 point-scanning confocal microscope. Five pre-bleach frames (1.29 seconds each) were recorded before bleaching with a 488-nm laser to achieve a bleach depth averaging 76%±7% (SD). Seventy-five post-bleach frames (1.29 seconds each) were then acquired. ROIs (1.25×3 µm) were placed over individual Z-discs and those with drift were discarded. For each fly, three Z-discs on different myofibrils were bleached, and intensities of adjacent unbleached Z-discs and unbleached background regions were recorded. Fluorescence was normalized as (bleached–background)/(unbleached– background), averaged across the three ROIs, and scaled such that the post-bleach frame equaled 0 and the pre-bleach mean equaled 100. Recovery curves were presented as mean±SEM. Each fly's curve was fitted to a one-phase

exponential association model to obtain the plateau (mobile fraction). Fixed samples were prepared in the same manner except with an additional ten-minute fixation in 4% paraformaldehyde in HL3 saline.

Microscopy

Confocal images were acquired using a HC PL APO 63×/1.40 OIL CS2 objective on a Leica SP8 point-scanning confocal microscope. The position along the z-axis was adjusted until perfectly in the centre of the myofibril, i.e., the widest point. Polarized light images were acquired using a 5X N-ACHROPLAN, NA=0.13 objective on a Zeiss Axio Observer microscope. TEM images were acquired using an FEI Tecnai G2 Spirit Twin 120 kV Cryo-TEM using an AMT NanoSprint15 MK2 CMOS camera.

Computational analyses

Schematics were illustrated with IBS 2.0 (Xie et al., 2022). All protein domains were defined per SMART (Letunic & Bork, 2018). Graphing and statistical analysis was performed using GraphPad Prism 10. Statistical analyses were performed in GraphPad Prism 10, where ns=$p \geq 0.05$, *=$p<0.05$; **=$p<0.01$, and ****=$p<0.0001$, and calculated to four decimal places. Equivalence of bend angles was assessed using the Two One-Sided Test (TOST) procedure. Model sarcomeres with bend angles ranging from 180° (straight) to 95° and blurring were generated. Each was hand measured ten times and the average absolute measurement error (4.5°) was used as the equivalence margin for all TOST analyses.

Minus strand RNA-seq bigWig files from the ENCODE project (Duff et al., 2015) with the following accessions were retrieved and loaded in IGV 2.19.4 (Robinson et al., 2011): ENCFF289ZZT, ENCFF982OGI, ENCFF430HWM, ENCFF716DNU, ENCFF829OGQ, ENCFF936YJM, ENCFF987YVI, ENCFF033MIY, ENCFF845HII, ENCFF021VXY, ENCFF792FNT. Signal tracks were aligned to the dm3 assembly and the data range was adjusted uniformly for all tracks.

SRA files with the following accession numbers were downloaded from the Bioproject PRJNA419412 (Spletter et al., 2018): SRR6314253, SRR6314256, SRR6314275, SRR6314259, SRR6314277, SRR6314262, SRR6314273. Salmon 1.10.0 (Patro et al., 2017) was used to quantify expression of the following transcripts which correspond to identified Zasp52 isoforms: FBtr0392902, FBtr0329914, FBtr0329912, FBtr0100387, FBtr0111048, FBtr0087315, FBtr0329913, FBtr0310086, FBtr0329916, FBtr0329915, FBtr0310088, FBtr0310087, FBtr0392901, FBtr0329911, FBtr0342711, FBtr0100388, FBtr0302163, FBtr0301313, FBtr0479884, FBtr0329909, FBtr0392918, FBtr0329910. The first six were classified as containing only exon 15a, the next six containing exons 15b-d, the next four containing exon 15e, and the last six containing no exon 15.

ImageJ was used to evaluate bending manually using the angle tool, and sarcomere length using the line measuring tool. For measuring patchiness, Niblack auto local thresholding of the actin channel using a radius of 15 units was performed, and outliers removed. The area of background within the myofibrils was divided by the area of the foreground thresholded selection to compute a patchiness metric.

For disorder prediction, the entire Zasp52-PF sequence was entered into AIUPred v0.1, DISOPRED3 (as two sequences, the first covering the first 1200 amino acids and the second, the remaining), or metapredict online v3.0. Raw values for each residue were obtained and smoothed using a Savitzky-Golay filter with fourth order smoothing and 11 neighbours on each side. AlphaFold v2.0 was used to obtain pLDDT scores for the alpha carbon of each residue. pLDDT scores were min-max normalized and smoothed in the same manner as above.

Zasp52 orthologs were obtained for members of the class *Insecta* using NCBI's Eukaryotic Genome Annotation Pipeline. Canonical protein sequences for each were downloaded and those which did not contain the classical PDZ and four LIM domains were removed. The number of residues between the first and second LIM domains was calculated. A phylogenetic tree of these species was created using NCBI's Common Tree (Schoch et al., 2020) and a heatmap created using iTOL v.6 (Letunic & Bork, 2024).

NARDINI (Cohan et al., 2022) was used for the sequences indicated to generate a z-score matrix, with 100,000 scrambled sequence variants.

Figure supplements

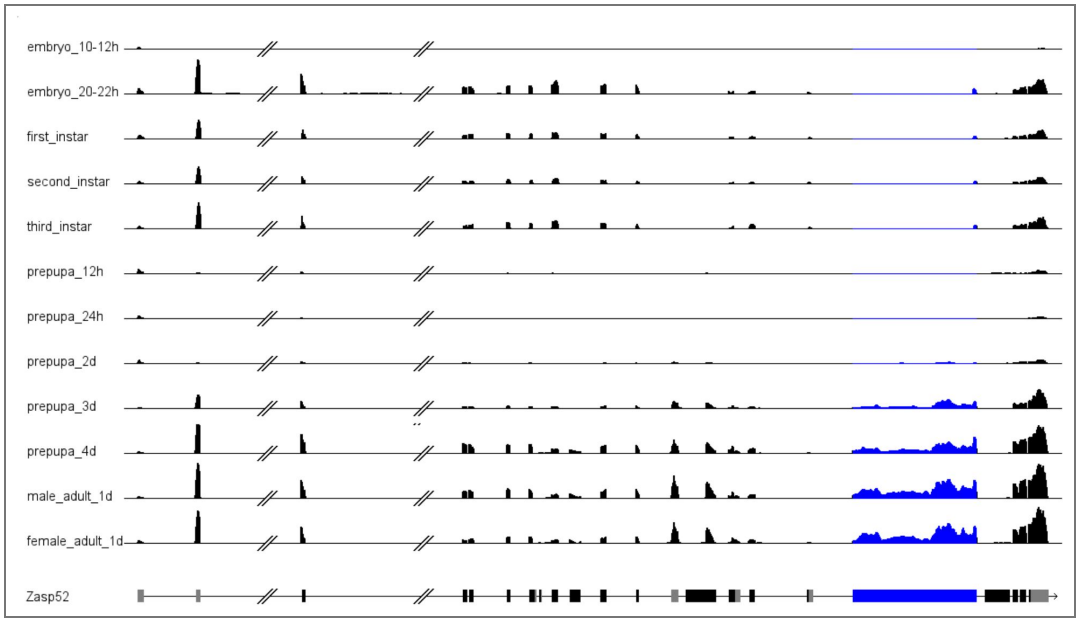

Supplementary Figure 1. MODENCODE RNA-seq data showing expression levels at the Zasp52 locus across various developmental stages. Exon 15e is highlighted in blue.

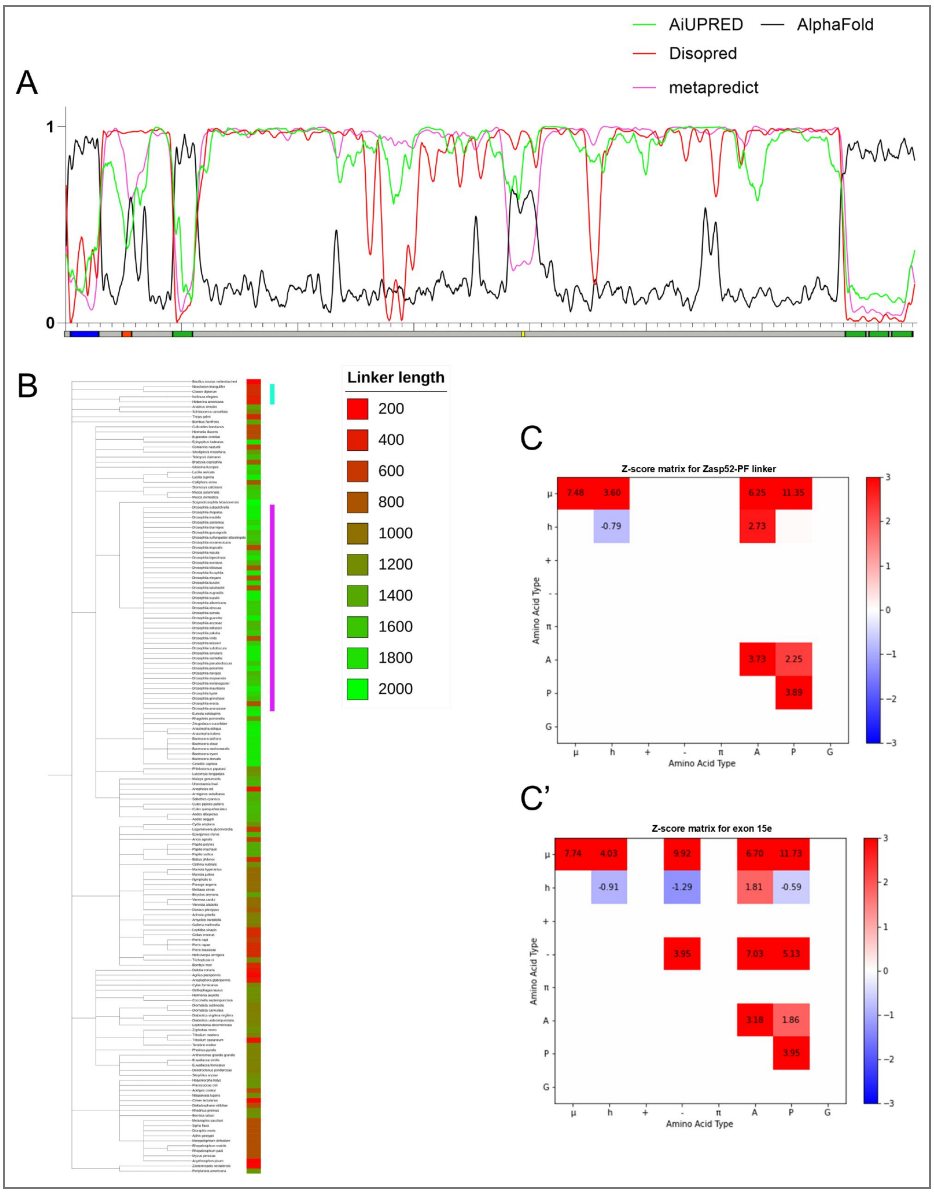

Supplementary Figure 2.

(A) Various disorder prediction algorithms were used to assess the level of per-residue disorder at the Zasp52 locus. The corresponding Zasp52 locus is schematized below, with PDZ domain (blue), ZM (red), LIM domains (green), and the ABM identified in Ashour et al., 2023 (yellow). For disorder prediction algorithms (AiUPRED, Disopred, and metapredict), the higher y-values represent higher levels of disorder while low values close to zero represent low levels of disorder (structure). AlphaFold pLDDT scores are plotted alongside in black. pLDDT scores can be used to inform about disorder with higher scores indicating higher confidence that a region is ordered, and lower scores suggesting disorder (Ruff & Pappu, 2021; Emenecker et al., 2021). **(B)** Dendrogram of various insects with Zasp52 orthologs that contain a PDZ domain and four LIM domains. Canonical isoforms which usually are also the longest ones were used to compute the number of residues comprising the linker between the first and second LIM domains, with data represented in a heatmap. The purple bar indicates all Drosophilids, and the teal bar indicates species of the order *Ephemeroptera* and *Odonata* which use direct flight. Though some Drosophilids contain shorter linkers, no other species contain linkers of comparable length to Drosophilids and other closely related Dipterans. NARDINI Z-score matrices of the linker region between LIM1 and LIM2 in Zasp52-PF **(C)** and of only the sequence encoded by exon 15e. The diagonal squares represent Ω-values which quantify the linear mixing versus segregation of all of residue type *x* with respect to all other residues. The off-diagonal squares represent δ-values which quantify the linear mixing versus segregation of pairs of residue types. A high z-score thus indicates segregation/blocking of a certain residue type with respect to itself/others compared to a null model; a low score indicates even dispersion and intermixing. Polar residues μ = {S,T,N,Q,C,H}; hydrophobic residues h = {I,L,V,M}; basic residues + = {R,K}; acidic residues - = {E,D}; aromatic residues π = {F,W,Y}; alanine = A; proline = P; glycine = G.

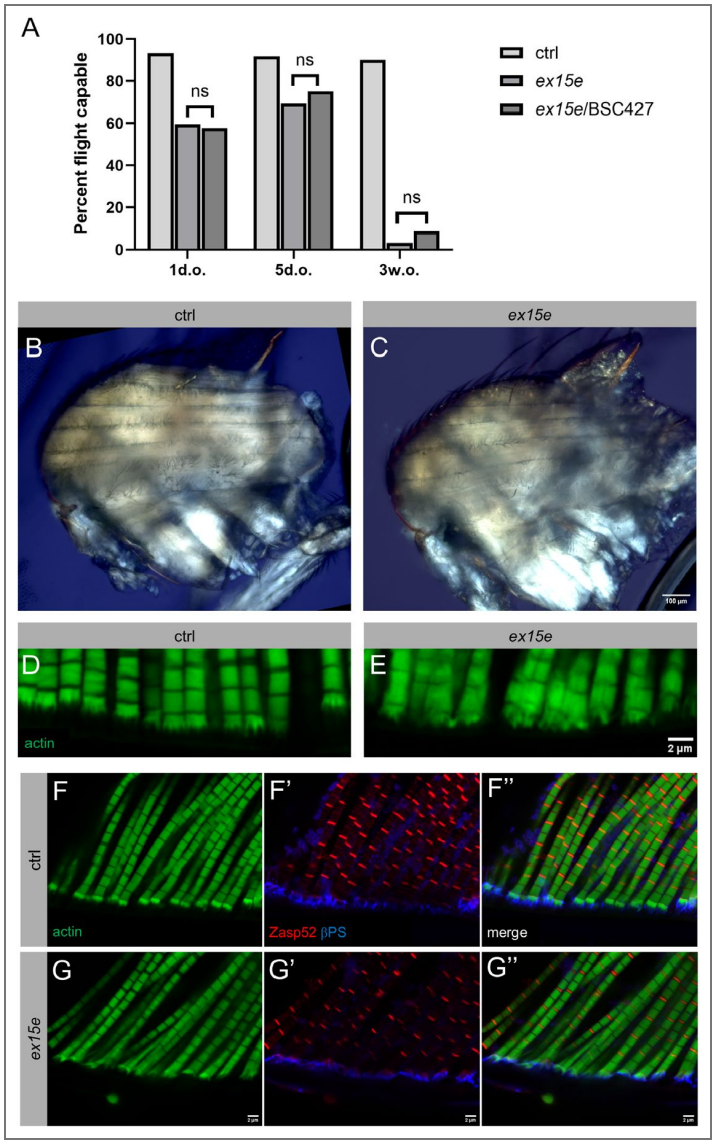

Supplementary Figure 3.

(A) A binary flight assay across three age categories of control, homozygous *ex15e*, and *ex15e* over a Zasp52 deficiency BSC427. Sample size were as follows: one-day-old (ctrl *n*=44 flies, *ex15e n*=42, *ex15e*/BSC427 *n*=45), five-days-old (ctrl *n*=48, *ex15e n*=39, *ex15e*/BSC427 *n*=28), and three-weeks-old (ctrl *n*=61, *ex15e n*=30, *ex15e*/BSC427 *n*=23). Flight was scored manually on whether they could generate upwards lift or not. There was no significant difference between the homozygous mutant or over the deficiency (Fisher's exact test; 1d.o. *p*=1.0000; 5d.o. *p*=0.7843; 3w.o. *p*=0.5729). Polarized light images of sagittally bisected thoraces of three-week-old control **(B)** and *ex15e* **(C)** revealed no obvious differences in gross morphology; females shown. **(D-G'')** MTZ were affected in *ex15e*. Close up views revealed a disruption in the MTZ and adjacent myofibrils in three-week-old *ex15e* mutants **(E)** compared to control **(D)**. The regular "crown"-shaped structure of the control MTZ is replaced with a disordered structure of variable shape in *ex15e* mutants. βPS integrin and Zasp52 localization appeared unaffected in *ex15e* **(F-G'')**. Thin filaments were visualized with phalloidin in green, Z-discs with a Zasp52 full-length antibody in red, and integrin adhesion sites at MTZs with a βPS integrin antibody in blue.

Acknowledgements

This work was funded by the Canadian Institutes of Health Research project grant PJT-178114. Confocal images were collected in the McGill University Advanced BioImaging Facility (ABIF). Electron microscopy images were collected and analyzed in the McGill University Facility for Electron Microscopy Research (FEMR).

Additional information

Funding

Funder	Grant reference number	Author
Canadian Institutes of Health Research (CIHR)	PJT-178114	Frieder Schöck

Author ORCID iDs

Frieder Schöck: https://orcid.org/0000-0002-1351-0574

References

Ashour D. J., Durney C. H., Planelles-Herrero V. J., Stevens T. J., Feng J. J., Röper K. (2023) Zasp52 strengthens whole embryo tissue integrity through supracellular actomyosin networks. *Development* **150** https://doi.org/10.1242/dev.201238 | PubMed

Babcock D. T., Ganetzky B. (2014) An Improved Method for Accurate and Rapid Measurement of Flight Performance in Drosophila. *Journal of Visualized Experiments* **84** https://doi.org/10.3791/51223 | PubMed

Benna C., Peron S., Rizzo G., Faulkner G., Migighian A., Perini G., Tognon G., Valle G., Reggiani C., Costa R., *et al.* (2009) Post-transcriptional silencing of the Drosophila homolog of human ZASP: a molecular and functional analysis. *Cell and Tissue Research* **337**:463-476 https://doi.org/10.1007/s00441-009-0813-y | PubMed

Bothe I., Baylies M. K. (2016) Drosophila myogenesis. *Current Biology* **26**:R786-R791 https://doi.org/10.1016/j.cub.2016.07.062 | PubMed

Brower D. L., Wilcox M., Piovant M., Smith R. J., Reger L. A. (1984) Related cell-surface antigens expressed with positional specificity in Drosophila imaginal discs. *PNAS* **81**:7485-7489 https://doi.org/10.1073/pnas.81.23.7485 | PubMed

Buchan D. W. A., Moffat L., Lau A., Kandathil S. M., Jones D. T. (2024) Deep learning for the PSIPRED Protein Analysis Workbench. *Nucleic Acids Research* **52**:W287-W293 https://doi.org/10.1093/nar/gkae328 | PubMed

Chechenova M. B., Bryantsev A. L., Cripps R. M. (2013) The Drosophila Z-disc Protein Z(210) Is an Adult Muscle Isoform of Zasp52, Which Is Required for Normal Myofibril Organization in Indirect Flight Muscles. *Journal of Biological Chemistry* **288**:3718-3726 https://doi.org/10.1074/jbc.m112.401794 | PubMed

Cohan M. C., Shinn M. K., Lalmansingh J. M., Pappu R. V. (2022) Uncovering Non-random Binary Patterns Within Sequences of Intrinsically Disordered Proteins. *Journal of Molecular Biology* **434** https://doi.org/10.1016/j.jmb.2021.167373 | PubMed

Cortese M. S., Uversky V. N., Dunker A. K. (2008) Intrinsic disorder in scaffold proteins: getting more from less. *Progress in Biophysics and Molecular Biology* **98**:85-106 https://doi.org/10.1016/j.pbiomolbio.2008.05.007 | PubMed

Duff M. O., Olson S., Wei X., Garrett S. C., Osman A., Bolisetty M., Plocik A., Celniker S. E., Graveley B. R. (2015) Genome-wide identification of zero nucleotide recursive splicing in Drosophila. *Nature* **521**:376-379 https://doi.org/10.1038/nature14475 | PubMed

Emenecker R. J., Griffith D., Holehouse A. S. (2021) Metapredict: a fast, accurate, and easy-to-use predictor of consensus disorder and structure. *Biophysical Journal* **120**:4312-4319 https://doi.org/10.1016/j.bpj.2021.08.039 | PubMed

Erdős G., Dosztányi Z. (2024) AIUPred: combining energy estimation with deep learning for the enhanced prediction of protein disorder. *Nucleic Acids Research* **52**:W176-W181 https://doi.org/10.1093/nar/gkae385 | PubMed

Fisher L. A. B., Schöck F. (2022) The unexpected versatility of ALP/Enigma family proteins. *Frontiers in Cell and Developmental Biology* **10** https://doi.org/10.3389/fcell.2022.963608 | PubMed

González-Morales N., Holenka T. K., Schöck F. (2017) Filamin actin-binding and titin-binding fulfill distinct dunctions in Z-disc cohesion. *PLoS Genetics* **13** https://doi.org/10.1371/journal.pgen.1006880 | PubMed

González-Morales N., Xiao Y.-S., Schilling M. A., Marescal O., Liao K. A., Schöck F. (2019) Myofibril diameter is set by a finely tuned mechanism of protein oligomerization in Drosophila. *eLife* **8** https://doi.org/10.7554/elife.50496 | PubMed

Griggs R., Vihola A., Hackman P., Talvinen K., Haravuori H., Faulkner G., Eymard B., Richard I., Selcen D., Engel A., *et al.* (2007) Zaspopathy in a large classic late-onset distal myopathy family. *Brain* **130**:1477-1484 https://doi.org/10.1093/brain/awm006 | PubMed

Healy M. D., Collins B. M. (2023) The PDLIM family of actin-associated proteins and their emerging role in membrane trafficking. *Biochemical Society Transactions* **15**:2005-2016 https://doi.org/10.1042/bst20220804 | PubMed

Huang C., Zhou Q., Liang P., Hollander M. S., Sheikh F., Li X., Greaser M., Shelton G., Evans S., Chen J. (2003) Characterization and in Vivo Functional Analysis of Splice Variants of Cypher. *Journal of Biological Chemistry* **278**:7360-7365 https://doi.org/10.1074/jbc.m211875200 | PubMed

Jani K., Schöck F. (2007) Zasp is required for the assembly of functional integrin adhesion sites. *Journal of Cell Biology* **179**:1583-1597 https://doi.org/10.1083/jcb.200707045 | PubMed

Jensen C. C., Gurley N. J., Mathias A. J., Wolfsberg L. R., Xiao Y., Zhou Z., Bischoff M. C., Clark S. E., Slep K. C., Peifer M. (2025) A key role of Canoe's intrinsically disordered region in linking cell junctions to the cytoskeleton. *Journal of Cell Biology* **224** https://doi.org/10.1083/jcb.202505135 | PubMed

Jones D. T., Cozzetto D. (2015) DISOPRED3: precise disordered region predictions with annotated protein-binding activity. *Bioinformatics* **31**:857-863 https://doi.org/10.1093/bioinformatics/btu744 | PubMed

Jumper J., Evans R., Pritzel A., Green T., Figurnov M., Ronneberger O., Tunyasuvunakool K., Bates R., Žídek A., Potapenko A., *et al.* (2021) Highly accurate protein structure prediction with AlphaFold. *Nature* **596**:583-589 https://doi.org/10.1038/s41586-021-03819-2 | PubMed

Katzemich A., Long J. Y., Jani K., Lee B. R., Schöck F. (2011) Muscle type-specific expression of Zasp52 isoforms in Drosophila. *Gene Expression Patterns* **11**:484-490 https://doi.org/10.1016/j.gep.2011.08.004 | PubMed

Katzemich A., Liao K. A., Czerniecki S., Schöck F. (2013) Alp/Enigma Family Proteins Cooperate in Z-Disc Formation and Myofibril Assembly. *PLoS Genetics* **9** https://doi.org/10.1371/journal.pgen.1003342 | PubMed

Krans J. L. (2010) The Sliding Filament Theory of Muscle Contraction. Nature Education.

Letunic I., Bork P. (2018) 20 years of the SMART protein domain annotation resource. *Nucleic Acids Research* **46**:D493-D496 https://doi.org/10.1093/nar/gkx922 | PubMed

Letunic I., Bork P. (2024) Interactive Tree of Life (iTOL) v6: recent updates to the phylogenetic tree display and annotation tool. *Nucleic Acids Research* **52**:W78-W82 https://doi.org/10.1093/nar/gkae268 | PubMed

Liao K. A., González-Morales N., Schöck F. (2016) Zasp52, a Core Z-disc Protein in Drosophila Indirect Flight Muscles, Interacts with α-Actinin via an Extended PDZ Domain. *PLoS Genetics* **12** https://doi.org/10.1371/journal.pgen.1006400 | PubMed

Liao K. A., González-Morales N., Schöck F. (2020) Characterizing the actin-binding ability of Zasp52 and its contribution to myofibril assembly. *PLoS ONE* **15** https://doi.org/10.1371/journal.pone.0232137 | PubMed

Lin X., Ruiz J., Bajraktari I., Ohman R., Banerjee S., Gribble K., Kaufman J. D., Wingfield P. T., Griggs R. C., Fischbeck K. H., *et al.* (2014) Z-disc-associated, Alternatively Spliced, PDZ Motif-containing Protein (ZASP) Mutations in the Actin-binding Domain Cause Disruption of Skeletal Muscle Actin Filaments in Myofibrillar Myopathy. *Journal of Biological Chemistry* **289**:13615-13626 https://doi.org/10.1074/jbc.m114.550418 | PubMed

Lotthammer J. M., Hernández-García J., Griffith D., Weijers D., Holehouse A. S., Emenecker R. J. (2024) Metapredict enables accurate disorder prediction across the Tree of Life. *bioRxiv* https://doi.org/10.1101/2024.11.05.622168

Nikonova E., Kao S.-Y., Spletter M. L. (2020) Contributions of alternative splicing to muscle type development and function. *Seminars in Cell & Developmental Biology* **104**:65-80 https://doi.org/10.1016/j.semcdb.2020.02.003 | PubMed

Patro R., Duggal G., Love M. I., Irizarry R. A., Kingsford C. (2017) Salmon provides fast and biasaware quantification of transcript expression. *Nature Methods* **14**:417-419 https://doi.org/10.1038/nmeth.4197 | PubMed

Post Y., Paululat A. (2018) Muscle Function Assessment Using a Drosophila Larvae Crawling Assay. *Bio-protocol* **8** https://doi.org/10.21769/bioprotoc.2933 | PubMed

Robinson J. T., Thorvaldsdóttir H., Winckler W., Guttman M., Lander E. S., Getz G., Mesirov J. P. (2011) Integrative Genomics Viewer. *Nature Biotechnology* **29**:24-26 https://doi.org/10.1038/nbt.1754 | PubMed

Ruff K. M., Pappu R. V. (2021) AlphaFold and Implications for Intrinsically Disordered Proteins. *Journal of Molecular Biology* **433** https://doi.org/10.1016/j.jmb.2021.167208 | PubMed

Rui Y., Bai J., Perrimon N. (2010) Sarcomere Formation Occurs by the Assembly of Multiple Latent Protein Complexes. *PLoS Genetics* **6** https://doi.org/10.1371/journal.pgen.1001208 | PubMed

Schoch C. L., Ciufo S., Domrachev M., Hotton C. L., Kannan S., Khovanskaya R., Leipe D., Mcveigh R., O'Neill K., Robbertse B., *et al.* (2020) NCBI Taxonomy: a comprehensive update on curation, resources and tools. *Database : the journal of biological databases and curation* https://doi.org/10.1093/database/baaa062 | PubMed

Selcen D., Engel A. G. (2005) Mutations in ZASP define a novel form of muscular dystrophy in humans. *Annals of Neurology* **57**:269-276 https://doi.org/10.1002/ana.20376 | PubMed

Spletter M. L., Barz C., Yeroslaviz A., Zhang X., Lemke S. B., Bonnard A., Brunner E., Cardone G., Basler K., Habermann B. H., *et al.* (2018) A transcriptomics resource reveals a transcriptional transition during ordered sarcomere morphogenesis in flight muscle. *eLife* **7** https://doi.org/10.7554/elife.34058 | PubMed

Steinmetz P. R. H., Kraus J. E. M., Larroux C., Hammel J. U., Amon-Hassenzahl A., Houliston E., Wörheide G., Nickel M., Degnan B. M., Technau U. (2012) Independent evolution of striated muscles in cnidarians and bilaterians. *Nature* **487**:231-234 https://doi.org/10.1038/nature11180 | PubMed

Stewart B. A., Atwood H. L., Renger J. J., Wu C. F. (1994) Improved stability of Drosophila larval neuromuscular preparations in haemolymph-like physiological solutions. *Journal of comparative physiology* **175**:179-191 https://doi.org/10.1007/bf00215114 | PubMed

Szikora S., Novák T., Gajdos T., Erdélyi M., Mihály J. (2020) Superresolution Microscopy of Drosophial Indirect Flight Muscle Sarcomeres. *Bio-protocol* **10** https://doi.org/10.21769/bioprotoc.3654 | PubMed

Varadi M., Anyango S., Deshpande M., Nair S., Natassia C., Yordanova G., Yuan D., Stroe O., Wood G., Laydon A., *et al.* (2022) AlphaFold Protein Structure Database: massively expanding the structural coverage of protein-sequence space with high-accuracy models. *Nucleic Acids Research* **50**:D439-D444 https://doi.org/10.1093/nar/gkab1061 | PubMed

Vatta M., Mohapatra B., Jimenez S., Sanchez X., Faulkner G., Perles Z., Sinagra G., Lin J.-H., Vu T. M., Zhou Q., *et al.* (2003) Mutations in Cypher/ZASP in patients with dilated cardiomyopathy and left ventricular non-compaction. *Journal of the American College of Cardiology* **42**:2014-2027 https://doi.org/10.1016/j.jacc.2003.10.021 | PubMed

Venken K. J. T., Schulze K. L., Haelterman N. A., Pan H., He Y., Evans-Holm M., Carlson J. W., Levis R. W., Spradling A. C., Hoskins R. A., *et al.* (2011) MiMIC: a highly versatile transposon insertion resource for engineering Drosophila melanogaster genes. *Nature methods* **8**:737-743 https://doi.org/10.1038/nmeth.1662 | PubMed

Watts N. R., Zhuang X., Kaufman J. D., Palmer I. W., Dearborn A. D., Coscia S., Blech-Hermoni Y., Alfano C., Pastore A., Mankodi A., *et al.* (2017) Expression and Purification of ZASP Subdomains and Clinically Important Isoforms: High-Affinity Binding to G-Actin. *Biochemistry* **56**:2061-2070 https://doi.org/10.1021/acs.biochem.7b00067 | PubMed

Xiao Y. S., Schöck F., González-Morales N. (2017) Rapid IFM Dissection for Visualizing Fluorescently Tagged Sarcomeric Proteins. *Bio-protocol* **7** https://doi.org/10.21769/bioprotoc.2606 | PubMed

Xie Y., Li H., Luo X., Li H., Gao Q., Zhang L., Teng Y., Zhao Q., Zuo Z., Ren J. (2022) IBS 2.0: an upgraded illustrator for the visualization of biological sequences. *Nucleic Acids Research* **50**:W420-W426 https://doi.org/10.1093/nar/gkac373 | PubMed

Zhou Q., Chu P.-H., Huang C., Cheng C.-F., Martone M. E., Knoll G., Shelton D., Evans S., Chen J. (2001) Ablation of Cypher, a PDZ-LIM domain Z-line protein, causes a severe form of congenital myopathy. *Journal of Cell Biology* **155**:605-612 https://doi.org/10.1083/jcb.200107092 | PubMed

Peer reviews

Reviewer #1 (Public review):

The manuscript by Ho and Schock investigates the role of the Z-disc protein Zasp52 during Drosophila flight muscle development. It was known before, mainly by findings from this group, that Zasp52 is required for normal sarcomere morphogenesis, specifically Z-disc morphogenesis in indirect flight muscles. But the exact molecular mechanism by which Zasp52 contributes, apart from the fact that it is localised there and is somehow involved in multimerization/cross-linking, was not clear. This paper proposes that an intrinsically disordered region (IDR) in Zasp52 is needed for some of its functions, by stabilising Zasp52 localisation at the Z-disc. Specifically, the IDR in Zasp52 is proposed to be required for Z-disc maintenance during the mechanical challenges of flight, while being dispensable for the initial morphogenesis during development. This hypothesis is supported by strong genetic evidence and behavioural tests, deleting Zasp's IDR impairs flight from mid-age onwards, while a block in flight activity lifts the phenotype.

However, some of the phenotypic analysis, in particular the bending of the sarcomere, likely upon mechanical challenge by muscle contractions, needs more detailed investigations to be fully convincing.

Strengths:

(1) The linker in the alternatively spliced exon 15 of Zasp52 was deleted with a state-of-the-art genetic editing strategy. Surprisingly, flies are homozygous viable, showing that this long part of the Zasp52 protein is not essential for animal survival or sarcomere morphogenesis.

(2) The observed sarcomere phenotypes with age, especially the bending Z-discs, are new and exciting.

(3) The displayed EM images document interesting phenotypes.

(4) Most of the observed phenotypes can be rescued by re-expression of the long Zasp52 isoform, which does contain the IDR region, but not by a shorter one without it, suggesting that IDR is important.

(5) FRAP data measure the local turnover of a short-ZaspGFP and show that this increased in the Zasp mutant lacking the IDR domain, suggesting that Zasp-IDR might stabilise Zasp at the Z-disc.

(6) Interestingly, flight and sarcomere morphology phenotypes can be rescued by preventing the flies from flying, suggesting that they are mechanically induced.

Weaknesses:

(1) The western blot quantifications of Zasp isoform expression are weak. No error bars are indicated in the quantifications; the quantifications appear to be more qualitative than quantitative. According to band intensities, the long Zasp isoforms seem to be less present compared to the shorter ones, even in the flight muscles.

(2) The phenotypic analysis of the sarcomere appears somewhat superficial throughout the paper. Only Zasp52 and phalloidin are shown; no other Z-disc or thick filament proteins. At least myosin stainings and overview images are important to better judge the phenotypic variations. Are the variants between individuals or regional in the same muscle?

(3) EM images would benefit from better quantification.

(4) Other proteins were not analysed with the FRAP-based turnover assay for comparison in wild type and mutant. All Z-proteins might turn over faster in the mutant with the defective Z-disc.

https://doi.org/10.7554/eLife.111101.1.sa2

Reviewer #2 (Public review):

Summary and Strengths:

This in-depth genetic analysis of Zasp52 function in Drosophila indirect flight muscle (IFM) provides an interesting perspective regarding the role of a partially disordered region (IDR) in exon 15e. This exon seems to be exclusively present in IFM and contributes to the prevention of myofibril disintegration during aging, likely due to interactions of this region with Z-disc insertion and/or stability. The addition of an isoform (PR) that lacks exon 15e serves as a nice control to illustrate the necessity of exon 15e in muscle structure and function. Overall, the manuscript is exceptionally well-written, logical, with nicely controlled experiments and detailed statistical analysis that largely support the conclusions drawn by the authors. While exon 15e is clearly involved in preventing muscle degeneration, a solid role for thin filament stability is not clearly shown (as mentioned in the abstract). In addition, which regions/how the proteins of the IDR may contribute are unclear.

Weaknesses:

(1) It is not clear in Figure S1A where exon 15e fits within the Zasp52 locus schematic. This is important as a premise of this paper describes this region to be key, and proof from multiple prediction programs would lend more weight to the prediction of the exon being largely disordered. Inclusion of the discussed short linear motifs, comparison with Canoe or LBD3 for similarities and/or an Alphafold structure would help make the authors' point (colorized with known domains).

(2) Interesting that immobilization rescues the deterioration phenotypes. The authors should explain in more detail how this was done to avoid dehydration/starvation of the flies.

(3) There is a lot of discussion about the potential function of the IDR region, specifically a putative actin binding motif or other 'ordered' regions that may contain short linear motifs. It would strengthen the findings to show which of these may be essential for Zasp52 function in the IFM. The ability to bind actin could be tested biochemically, and/or smaller deletions could be made to unequivocally test the role of the ABD vs other predicted motifs using genetics. If some of these regions are more ordered, where do they lie within, and do they form a predicted fold or structure that gives insight into function?

https://doi.org/10.7554/eLife.111101.1.sa1

Author response:

Public Reviews:

Reviewer #1 (Public review):

The manuscript by Ho and Schock investigates the role of the Z-disc protein Zasp52 during Drosophila flight muscle development. It was known before, mainly by findings from this group, that Zasp52 is required for normal sarcomere morphogenesis, specifically Z-disc morphogenesis in indirect flight muscles. But the exact molecular mechanism by which Zasp52 contributes, apart from the fact that it is localised there and is somehow involved in multimerization/cross-linking, was not clear. This paper proposes that an intrinsically disordered region (IDR) in Zasp52 is needed for some of its functions, by stabilising Zasp52 localisation at the Z-disc. Specifically, the IDR in Zasp52 is proposed to be required for Z-disc maintenance during the mechanical challenges of flight, while being dispensable for the initial morphogenesis during development. This hypothesis is supported by strong genetic evidence and behavioural tests, deleting Zasp's IDR impairs flight from mid-age onwards, while a block in flight activity lifts the phenotype.

However, some of the phenotypic analysis, in particular the bending of the sarcomere, likely upon mechanical challenge by muscle contractions, needs more detailed investigations to be fully convincing.

Strengths:

(1) The linker in the alternatively spliced exon 15 of Zasp52 was deleted with a state-of-the-art genetic editing strategy. Surprisingly, flies are homozygous viable, showing that this long part of the Zasp52 protein is not essential for animal survival or sarcomere morphogenesis.

(2) The observed sarcomere phenotypes with age, especially the bending Z-discs, are new and exciting.

(3) The displayed EM images document interesting phenotypes.

(4) Most of the observed phenotypes can be rescued by re-expression of the long Zasp52 isoform, which does contain the IDR region, but not by a shorter one without it, suggesting that IDR is important.

(5) FRAP data measure the local turnover of a short-ZaspGFP and show that this increased in the Zasp mutant lacking the IDR domain, suggesting that Zasp-IDR might stabilise Zasp at the Z-disc.

> *(6) Interestingly, flight and sarcomere morphology phenotypes can be rescued by preventing the flies from flying, suggesting that they are mechanically induced.*
>
> *Weaknesses:*
>
> *(1) The western blot quantifications of Zasp isoform expression are weak. No error bars are indicated in the quantifications; the quantifications appear to be more qualitative than quantitative. According to band intensities, the long Zasp isoforms seem to be less present compared to the shorter ones, even in the flight muscles.*

We will work on including quantifications with error bars for the Western blots in our resubmission. It is important to keep in mind that the main point in figure 1B is that there are plenty of exon15e-containing isoforms in IFM, in contrast to other tissues with very limited exon15e-containing isoforms. This is confirmed by the analysis of RNAseq data in figure 1C, and of course, by the flightless phenotype of the exon15e mutant.

> *(2) The phenotypic analysis of the sarcomere appears somewhat superficial throughout the paper. Only Zasp52 and phalloidin are shown; no other Z-disc or thick filament proteins. At least myosin stainings and overview images are important to better judge the phenotypic variations. Are the variants between individuals or regional in the same muscle?*

Our images are representative of the observed phenotypes. We aim to provide overview images and other stainings to better illustrate the phenotypic variations in the revised version. Phenotypes are consistently present across all individuals, as reflected in our replicates. Interestingly, they appear to not be randomly interspersed among the sarcomeres but concentrated in certain regions of muscle more than others.

> *(3) EM images would benefit from better quantification.*

We do not believe that EM images can be meaningfully quantified, because of the many selection steps preceding image acquisition.

> *(4) Other proteins were not analysed with the FRAP-based turnover assay for comparison in wild type and mutant. All Z-proteins might turn over faster in the mutant with the defective Z-disc.*

This is the point we are trying to make. The Zasp52 IDR acts like a glue stabilizing all Z-disc proteins. We performed this experiment as a first step to explore whether an exon15e-lacking system exhibited modified dynamics, and we aim to provide more data in the revised version.

> ***Reviewer #2 (Public review):***
>
> *Summary and Strengths:*
>
> *This in-depth genetic analysis of Zasp52 function in Drosophila indirect flight muscle (IFM) provides an interesting perspective regarding the role of a partially disordered region (IDR) in exon 15e. This exon seems to be exclusively present in IFM and contributes to the prevention of myofibril disintegration during aging, likely due to interactions of this region with Z-disc insertion and/or stability. The addition of an isoform (PR) that lacks exon 15e serves as a nice control to illustrate the necessity of exon 15e in muscle structure and function. Overall, the manuscript is exceptionally well-written, logical, with nicely controlled experiments and detailed statistical analysis that largely support the conclusions drawn by the authors. While exon 15e is clearly involved in preventing muscle degeneration, a solid role for thin filament stability is not clearly shown (as*

> *mentioned in the abstract). In addition, which regions/how the proteins of the IDR may contribute are unclear.*
>
> *Weaknesses:*
>
> *(1) It is not clear in Figure S1A where exon 15e fits within the Zasp52 locus schematic. This is important as a premise of this paper describes this region to be key, and proof from multiple prediction programs would lend more weight to the prediction of the exon being largely disordered. Inclusion of the discussed short linear motifs, comparison with Canoe or LBD3 for similarities and/or an Alphafold structure would help make the authors' point (colorized with known domains).*

We will add a bar below figure S2A to show the region corresponding to exon 15e. We used three disorder prediction programs and one structure (order) prediction program. The majority of exon15e is completely disordered and of very low confidence score, and thus uninformative to display as an Alphafold structure. Likewise, IDR's are very difficult to classify, therefore we cannot say much more than that LDB3, Zasp52, and Canoe contain IDRs, with Zasp52 and Canoe both having an actin-binding domain within the IDR. We will provide more data on the function of the ABD in the revised version.

> *(2) Interesting that immobilization rescues the deterioration phenotypes. The authors should explain in more detail how this was done to avoid dehydration/starvation of the flies.*

We will provide more details in the revised version.

> *(3) There is a lot of discussion about the potential function of the IDR region, specifically a putative actin binding motif or other 'ordered' regions that may contain short linear motifs. It would strengthen the findings to show which of these may be essential for Zasp52 function in the IFM. The ability to bind actin could be tested biochemically, and/or smaller deletions could be made to unequivocally test the role of the ABD vs other predicted motifs using genetics. If some of these regions are more ordered, where do they lie within, and do they form a predicted fold or structure that gives insight into function?*

We will provide data on the function of the ABD in the revised version.

https://doi.org/10.7554/eLife.111101.1.sa0